2017

Efficient Energy Optimization for Smart Grid and Smart Community

Avijit Das
South Dakota State University

EFFICIENT ENERGY OPTIMIZATION FOR SMART GRID AND SMART COMMUNITY

BY

AVIJIT DAS

A thesis submitted in partial fulfillment of the requirements for the

Master of Science

Major in Electrical Engineering

South Dakota State University

2017

EFFICIENT ENERGY OPTIMIZATION FOR SMART GRID AND SMART COMMUNITY

This thesis is approved as a creditable and independent investigation by a candidate for the Master of Science in Electrical Engineering degree and is acceptable for meeting the thesis requirements for this degree. Acceptance of this thesis does not imply that the conclusions reached by the candidates are necessarily the conclusions of the major department.

Zhen Ni, Ph.D.
Thesis Advisor Date

Steven Hietpas, Ph.D.
Head, Electrical Engineering and Computer Science Date

Dean, Graduate School Date

ACKNOWLEDGEMENTS

Foremost, I would like to express the deepest gratitude to my advisor, Dr. Zhen Ni. I have been amazingly fortunate to have an advisor who gave me the freedom to explore on my own, and at the same time the guidance to recover when my steps faltered. Being his student is and always will be one of the greatest honors of my life. Dr. Ni gave many constructive suggestions in my study and his instructions paved the way to this dissertation. In addition, he taught me many skills in writing and revising manuscripts.

Besides my advisor, I would like to thank the rest of my thesis committee: Dr. Timothy M. Hansen for their insightful comments and constructive criticism at different stages of my research. I am grateful to Dr. Qiquan Qiao for practical advice and comments on the countless revision of this manuscript. In addition, many thanks to the graduate faculty representative Dr. Johan Osorio for his valuable time.

I am also indebted to my friends, Tamal, Shuva, Naresh, Venkat, Shiva, and many others. They have helped me stay sane through these difficult years and their support helped me overcome setbacks and stay focused on my graduate study.

Finally, I must express my very profound gratitude to my parents and my spouse, Nila, for providing me with unfailing support and continuous encouragement throughout my years of study and through the process of researching and writing this thesis. Last but not the least, I love my son Areejit who is the most precious gift from God and whose love I can never thank enough.

CONTENTS

ABBREVIATIONS

SOC	State of Charge
SOC_{stp}	Set-up State of Charge
ADP	Approximate Dynamic Programming
BESS	Battery Energy Storage System
CC	Charge Controller
CEMS	Community Energy Management System
DER	Distributed Energy Resource
DP	Dynamic Programming
DR	Demand Response
DRR	Demand Reduction Request
DSM	Demand Side Management
IBDR	Incentive Based Demand Response
LP	Linear Programming
MDP	Markov Decision Process
PBDR	Price Based Demand Response
RES	Renewable Energy Source
SBSP	Scenario Based Stochastic Programming

LIST OF FIGURES

LIST OF TABLES

ABSTRACT

EFFICIENT ENERGY OPTIMIZATION FOR SMART GRID AND SMART COMMUNITY

AVIJIT DAS

2017

The electric power industry has undergone significant changes in response to the environmental concerns during the past decades. Nowadays, due to the integration of different distributed energy systems in the smart grid, the balancing between power generation and load demand becomes a critical problem. Specifically, due to the intermittent nature of renewable energy sources (RESs) , power system optimization becomes significantly complicated. Due to the uncertain nature of RESs, the system may fail to ensure the power quality which may cause increased operating costs for committing costly reserve units or penalty costs for curtailing load demands. This dissertation presents three projects to study the optimization and control for smart grid and smart community.

First, optimal operation of battery energy storage system (BESS) in grid-connected microgrid is studied. Near optimal operation/allocation of the BESS is investigated with the consideration of battery lifetime characteristics. Approximate dynamic programming (ADP) is proposed to solve optimal control policy for time-dependent and finite-horizon BESS problems and performance comparison is done with classical dynamic programming approach. The results show that the ADP can optimize the system operation under different scenarios to maximize the total system revenue.

Second, optimal operation of the BESS in islanded microgrid is also studied.

Specifically, a new islanded microgrid model is formulated based on Markov decision process. A computationally efficient ADP approach is proposed to solve this energy optimization problem, and achieve near minimum operational cost efficiently. Simulation results show that the proposed ADP can achieve 100% and at least 98% of optimality for deterministic and stochastic case studies, respectively. The performance of the proposed ADP approach also achieved 18.69 times faster response than that of the traditional DP approach for 0.5 million of data samples.

Third, a demand side management technique is proposed for the optimization of residential demands with financial incentives. A new design of comfort indicator is proposed considering both thermal and other electric appliances based on consumers' comfort level. The proposed approach is compared with two existing demand response approaches for both 10-houses and 100-houses simulation studies. For both cases, the proposed approach outperformed the existing approaches in terms of reward incentives and comfort levels.

CHAPTER 1 INTRODUCTION

1.1 Background

Global electricity generation is changing dramatically across the world due to the rising concerns of global climate change and volatile fossil fuel prices. During the past decades, due to the environmental concerns and energy crisis, distributed energy resources (DERs) such as renewable energy sources (RESs) are developed rapidly around the world. Though, the RESs are accepted as an environmentally and economically beneficial solution for future smart grids, however, the uncertain and intermittent output power of RESs poses many challenges for the power system such as power quality and system reliability [1]. The concept of microgrid is introduced to solve this problem which can be defined as an integrated system composed of the DERs, energy storage, and local loads, managed by an intelligent energy management system [2]. Basically, in microgrid, it has two modes of operation such as grid-connected mode and standalone or islanded mode. The grid-connected microgrid can be described as a microgrid which has inter-connection with the utility grid where the utility grid is used to maintain the system stability and reliability. On the other hand, the isolated or islanded microgrid can be defined as a small scale microgrid which has limited capacity to fulfill the load demand where the conventional generators and/or battery systems are used to increase the efficiency of the power supply by smoothing load fluctuations.

In recent years, for more efficient, reliable and environmentally friendly energy production, different energy sources are integrated into the microgrid. However, due to the integration of different energy systems in the microgrid, the balancing between power

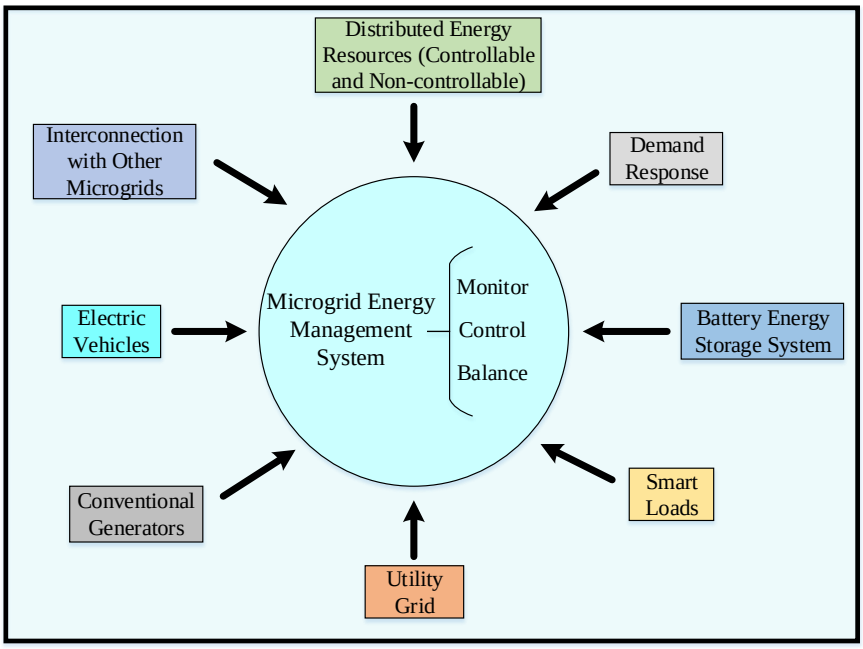

Figure 1.1. A general schematic diagram of microgrid energy management system with possible solutions.

generation and load demand becomes a critical problem. Specifically, the increasing penetration of uncertain and unpredictable RESs are introducing more uncertainties to power systems due to their uncertain behavior. Even a small error in forecasting may cause in great uncertainties for real-time operations of a microgrid. The mismatch between the forecasted power and the realized power may result in extra operating costs for committing costly reserve units or penalty cost for curtailing demand [3]. Also, Due to the stochastic nature of the RESs, the deterministic optimization may fail to ensure the power quality of the microgrid in an uncertain environment [4]. Therefore, in this research work, the stochastic nature of the RESs has been taken under consideration.

Nowadays, for reliable and satisfactory operation of the power systems, the power system optimization becomes an unavoidable issue [5]. In searching for viable solutions, scholars around the world have devoted significant efforts on the optimal operation of

microgrid, including integration of battery energy storage system (BESS) , demand response or demand management, interconnection with external grids, etc. [6]. Figure 1.1 schematically depicts the possible solutions for energy optimization in microgrid.

Amongst all the possible solutions, BESS has been recognized as one of the practically appealing solution to smooth out the power fluctuations in the renewable energy generation, thus improving both the reliability and efficiency of the microgrid [7]. For better utilization of the RESs in the microgrid, it is often desired to control and coordinate the BESS units in an efficient and economical way. Again, in the islanded microgrid, it is uneconomical to replace the BESS frequently due to transportation and labor cost [8]. Therefore, in recent years, it brings more attention to find an approach for the optimal operation of energy systems in the islanded microgrid with the consideration of the battery lifetime characteristics in the field of power system optimization.

Demand side management (DSM) is another widely used optimization technique for the microgrid. The main objective of DSM is to encourage users to consume less power during peak hours or to shift energy use to off-peak hours to flatten the load demand curve [9]. According to [10], in the U.S.A., residential load demands consume 38% of total electricity energy consumption. Residential demand-side resources have the potential to participate for improving the power system operation. There are 55 utility companies all over the U.S.A. offering the incentive based demand response (DR) programs to their residential customers [11]. The incentive based demand response program is a DSM technique where the participants are financially rewarded according to their quantified contributions in the DSM events. It can also be described as incentive payment program to reduce usage of electricity energy when the grid reliability is jeopardised [12]. In recent

years, due to the development of the DSM programs, the utility companies start to conduct pilots of incentive based demand response programs on intelligent loads to explore the possibility of increasing their revenues by aggregating residential demands. However, the consumers of these programs report that their comfort levels were affected. Also, existing reward systems are failed to attract more DR program participants. Therefore, in this research work, an advanced reward system and the concept of power consumption based comfort indicator are introduced to addressed the limitations of the existing approaches.

1.2 Literature Review on Energy Optimization of Microgrid with BESS

In the past decades, most of the existing literature focuses on deterministic microgrid operations [13]–[23]. To consider the intermittent nature of the RESs, the stochastic optimization methods have been widely researched for bulk power systems where the promising results are demonstrated by capturing the uncertainty associated with the RESs and considering worst-case scenarios [24]–[27]. However, the energy optimization of microgrid using stochastic methods has not been well documented in the existing literature [4]. Due to the stochastic nature of the RESs, the deterministic optimization may fail to ensure the power quality of the microgrid in an uncertain environment. In addition, most of the previous studies have assumed constant efficiency and zero operating cost for the BESS [4], [28]–[32]. Therefore, in this work, the uncertain nature of the RESs and the operating cost of the BESS with the analysis of battery lifetime characteristics have been taken under consideration.

In the field of stochastic optimization of power systems, several studies are based on scenario-based stochastic programming (SBSP) [4], [31]–[36]. However, the existing

literature has reported that the computation time for the SBSP depends on the number of scenarios. With large number of scenarios, the system would impose considerable computational cost. In recent years, many researchers have proposed different scenario reduction techniques to make the SBSP faster. However, this scenario reduction techniques may overlook low-probability but high-impact scenarios. Another widely used technique is called particle swarm optimization (PSO). In [1], [37]–[39], the PSO techniques have been investigated for the optimal operation of energy systems in the microgrid. However, the PSO techniques may fall into local optimal solution due to the problem of premature [40].

In recent years, for the islanded microgrid, the problem of finding optimal control policies for the operation in the BESS considering battery lifetime characteristics, is becoming increasingly important. In this work, for the analysis of lifetime characteristics of the BESS, a state of charge (SOC) based operation strategy is used where the battery is operated at a certain range of SOC. The other battery parameters, which have significant effects on the battery lifetime like maximum charging and discharging rate, maximum charging and discharging efficiency and maximum capacity, are also taken into account.

Most of the time, sequential decision problems with stochastic variables are modeled as stochastic dynamic programs. However, when state space becomes large, conventional techniques like backward dynamic programming, policy iteration, value iteration, etc., become computationally intractable [41]. This situation is known as the "curse of dimensionality" [42]. The approximate dynamic programming (ADP) is a technique to solve these problems approximately very close to the optimal point, with significantly fewer computational resources. In recent years, ADP is also considered as a

powerful tool for solving optimal control policies and attracts a lot of researcher's attention [43]. An ADP-based technique has been proposed for analysing the economic operation of BESS that has formulated as an optimization problem in [44]. In [45], the authors have investigated an ADP approach for the optimal control and allocation problem of a multidimensional energy storage system. In [46] and [47], the authors have applied ADP based control design for multi-bus power system stability and control with consideration of different disturbances. In microgrid, the BESS is one of the key components to store/provide energy. To achieve reliable and economic operation of the microgrid, in this work, the lifetime characteristics of BESS are fully investigated, and a battery control strategy for *SOC* is proposed to increase the battery lifetime and total yearly net savings in dollars.

1.3 Literature Review on Incentive Based Demand Response Program

In the existing literature, DR has been classified into price-based demand response (PBDR) and incentive-based demand response (IBDR) programs [12]. Conventionally, various types of PBDR programs have been proposed, such as time-of-use (TOU), critical peak pricing (CPP), peak load reduction pricing (PLRP), and real-time pricing (RTP) [33], [48]–[56]. Under these programs, the risks of the fluctuating wholesale electricity price are imposed upon retail customers in a mandatory manner. Most retail customers are risk-averse and they are not used to making decisions about electricity consumption on a daily or hourly basis. Also, equity problems might arise from time-dependent retail rate schemes, such as the day shift versus the night shift. Because of these issues, though the PBDR programs are theoretically attractive, however, time-varying retail rate schemes still

face obstacles in many regions when it comes to large-scale deployment [57].

According to [58], the IBDR programs are responsible for 93% of peak load reduction in the U.S. today. Many utility companies are implementing the IBDR programs to explore the possibility of increasing their profits by aggregating residential demands [59], [60]. However, the existing reward systems are not sufficiently attracting more DR program participants and the participants are also reported that their comfort levels were affected [11]. In [11], [61], [62], the different approaches are proposed to control the aggregated demand of air conditioners by adjusting their temperature settings. Most of the existing literatures are proposed different methodologies to minimize the peak hour load demands, to minimize the operational cost of the utilities and to maximize the benefits of the program participants [59], [63]–[65]. However, the energy consumption preferences and comfort levels of the users while minimizing the total reward cost of the utility have not been well-documented in the literature.

1.4 Motivations and Contributions

Nowadays, due to the increasing penetration of variable RESs, power system optimization becomes complicated for microgrid. As described in the literature review section, the stochastic optimization methods have been widely researched in transmission-level energy management system, however, the stochastic optimization for microgrid energy systems has not been well documented in the literature. Again, since, the BESS is one of the major power supply units in the microgrid, it is desired to control and coordinate the BESS in an efficient and economical way. In this work, first, a stochastic optimization problem for grid-connected microgrid is formulated as a Markov

decision process (MDP) where the near optimal operation/allocation problem of the BESS is investigated considering battery lifetime characteristics. The problem is formulated as a single objective optimization to maximize the total system revenue by considering the lifetime characteristics of lead-acid batteries. The ADP is proposed to solve optimal control policy for time-dependent and finite-horizon BESS problems. A classical dynamic programming approach has also been studied to validate the proposed approach. In addition, the real-time price data is used with different battery state of charge (*SOC*) to investigate the effect of lead-acid battery lifetime characteristics on the total system revenue.

Basically, in the islanded microgrid, the power generation capacity are limited. The distributed energy sources are the key power resources in islanded microgrid, especially in remote areas. In islanded microgrid, the uncertain behavior of the DERs presents many challenges in power generation and load balance maintenance to ensure power network stability and reliability. Also, in islanded microgrids, it is a challenge to optimize the BESSs with other power supply units (e.g., DERs and traditional power generator) and achieve the minimum daily operational cost. In this work, a new islanded microgrid model is formulated based on MDP. An ADP approach is proposed to solve the energy optimization problem, and to achieve near minimum operational cost efficiently. A battery control strategy is proposed to control and coordinate the BESS operation efficiently. The traditional linear programming (LP) and dynamic programming (DP) approaches are used to validate the percentage of optimality of the proposed approach for deterministic and stochastic case studies, respectively. The results show that the proposed approach can obtain 100% optimality in deterministic cases comparing with results from LP, and can

obtain competitive percentages of optimality with around 50% less computational time in stochastic cases comparing with results from DP. Moreover, the results verify that discharging the BESS at a certain *SOC* range can increase the battery lifetime and the yearly net savings of the system. In addition, the proposed approach is validated for different sets of large data samples and achieve 18.69 times faster response than that of the traditional DP approach for 0.5 million of data samples.

The DSM is one of the widely researched techniques for future smart grid in the field of power system optimization. It receives increasing attention by power research and industry due to its potential to improve the efficiency and quality of the power systems. However, the existing DSM strategies are failed to attract the customers sufficiently. Also, the users are also reported their inconvenience with the existing DSM strategies due to the violation of their comfort level. In this work, a residential community energy management system (CEMS) is proposed for the IBDR program users to allocate demand reduction requests (DRRs) among residential appliances efficiently without affecting their comfort levels and to reward residential consumers based on their actual participation. An advanced reward system is proposed to minimize the total reward costs for the utility and to distribute financial rewards according to the contributions of the users in the DR events. Also, a concept of comfort indicator was proposed to measure the comfort level of the residents where both thermal and other electric appliances are taken under consideration. The extensive simulation results validate the performance of the proposed approach. The proposed approach is also compared with two existing approaches and, for all cases, the proposed optimization approach outperformed the existing approaches.

1.5 The Structure of Thesis

The rest of the thesis is organized as follows. In Chapter 2, the stochastic power system optimization for grid-connected microgrid considering battery lifetime characteristics is discussed. A detailed description of the simulated model and performance comparison of the proposed approach with the traditional approach are provided. Chapter 3 briefly describes the performance of the proposed ADP approach for optimizing the BESS in islanded microgrid in both deterministic and stochastic environments. Chapter 4 discusses an efficient residential demand optimization scheme to optimize the residential load demands with the consideration of users' comfortability and to minimize the total reward costs for the utility. Finally, conclusions of the thesis and possible future works are presented in Chapter 5.

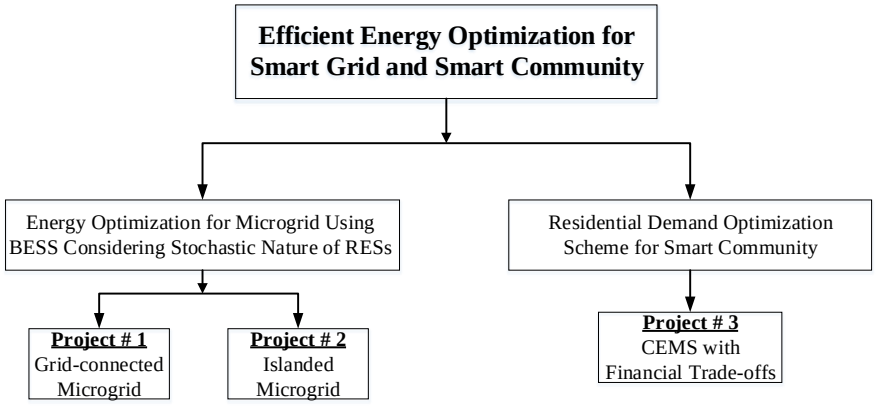

Figure 1.2. The structure of thesis.

CHAPTER 2 Near Optimal Control for Grid-connected Microgrid Energy Systems

2.1 Introduction

Due to the stochastic nature of RESs, the power system optimization becomes a critical issue. In searching for viable solutions, BESS has been recognized as one of the practically appealing solution to smooth out the power fluctuations in the renewable energy generation, thus improving both the reliability and efficiency of the microgrid. In this chapter, the near optimal operation of the BESS is studied with the presence of wind energy, load demand and power grid where the intermittent nature of wind energy is taken under consideration. The contribution of this chapter is threefold, (a) the near optimal operation/allocation problem of BESS for grid-connected microgrid system is addressed considering battery lifetime characteristics, (b) the proposed ADP algorithm is evaluated for stochastic datasets and compared with traditional dynamic programming (DP), (c) real-time price data is used with different battery SOC to investigate the effect of lead-acid battery lifetime characteristics on the total system revenue.

2.2 Problem Formulation

2.2.1 Grid-Connected Microgrid Model and Revenue Calculation

The optimal energy storage operation and allocation problem for grid-connected microgrid system are formulated as a MDP. The problem of allocating energy to a single grid-level storage device is considered over a finite horizon of time as $\tau = \{0, \Delta t, 2\Delta t, ..., T - \Delta t, T - 1\}$, where $\Delta t = 1$ is the time step and $T = 25$. The benchmark problem is illustrated in Figure 2.1.

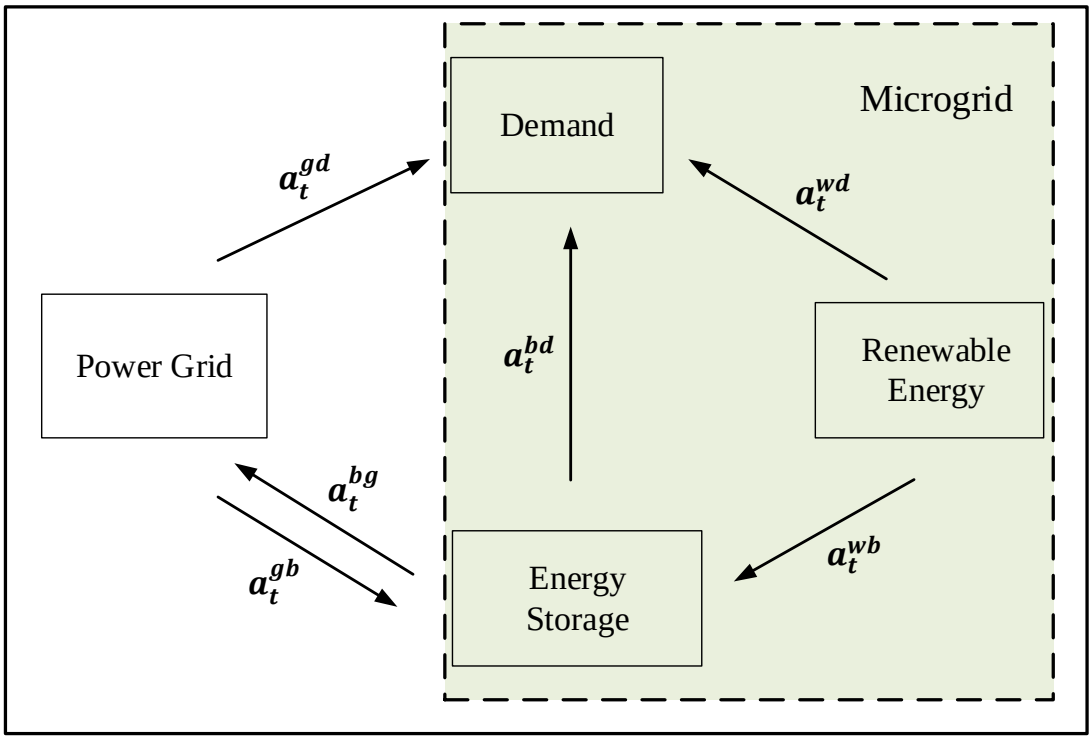

Figure 2.1. The power system model diagram for grid-connected microgrid, where the solid lines represent the transferred energy among components.

In the model, the microgrid is designed with an energy storage device that is connected with a wind farm and load demand as well as the main power grid. The actions are representing the flow of electricity that may flow directly from the wind farm to the storage device or it may be used to satisfy the load demand. Energy from storage may be sold to the grid at any given time and electricity from the grid may be bought to replenish the energy in storage or to satisfy the demand [45].

The following is a list of parameters used throughout the paper to characterize the storage device as,

- B^c: The energy capacity of the storage device, in MWh.
- ϕ^c: The charging efficiency of the device.

- ϕ^d: The discharging efficiency of the device.
- ψ^c: The maximum charging rates of the device, in $MWh/\Delta t$.
- ψ^d: The maximum discharging rates of the device, in $MWh/\Delta t$.

The state variable of the system at any time instance t can be written as,

$$S_t = (B_t, W_t, P_t, D_t). \tag{2.1}$$

- B_t: The amount of energy in the storage device, in MWh.
- W_t: The net amount of wind energy available, in MWh.
- P_t: The price of electricity in the power market, in $\$/MWh$.
- D_t: The aggregate energy demand, in MWh.

To be abbreviated, let E_t= (W_t,P_t,D_t) and S_t = (B_t,E_t), where E_t is the vector which contains exogenous information and E_t is independent of B_t. Next if the exogenous information, e_{t+1}, to be the change in E_t as,

$$E_{t+1} = E_t + e_{t+1}. \tag{2.2}$$

where, between time t and $t+1$, e_{t+1} = (w_{t+1},p_{t+1},d_{t+1}); The exogenous information e_{t+1} is independent of S_t and a_t.

- w_{t+1}: The change in the renewable energy.

- p_{t+1}: The change in the grid electricity price.
- d_{t+1}: The change in the load demand.

At any point of time t, the decision problem is that, while anticipating the future value of storage, the energy from the following three sources must need to be combined in order to fully satisfy the demand:

- The energy currently in storage, constrained by ψ^c, ψ^d, and B_t is represented by a decision a_t^{bd}.
- The available wind energy, constrained by E_t is represented by a decision a_t^{wd}.
- The energy from the grid, at a grid price of P_t is represented by a decision a_t^{gd}.

Additional allocation decisions are a_t^{bg}, the amount of storage energy to sell to the grid at price P_t; a_t^{wb}, amount of wind energy to transfer to the energy storage; and a_t^{gb}, the amount of energy to buy from the grid and store. These allocation decisions are summarized by the six-dimensional, nonnegative decision vector as,

$$a_t = (a_t^{wd}, a_t^{gd}, a_t^{bd}, a_t^{wb}, a_t^{gb}, a_t^{bg})^{\tau} \geq 0, a_t \in \chi_t \tag{2.3}$$

where, $t \in \tau$, χ_t represents feasible action space.

And the constraints are as follows:

$$a_t^{wd} + \phi^d a_t^{bd} + a_t^{gd} = D_t. \tag{2.4}$$

$$a_t^{bd} + a_t^{bg} \leq B_t. \tag{2.5}$$

$$a_t^{wb} + a_t^{gb} \leq B^c - B_t, \tag{2.6}$$

$$a_t^{wb} + a_t^{wd} \leq W_t. \tag{2.7}$$

$$a_t^{wb} + a_t^{gb} \leq \psi^c. \tag{2.8}$$

$$a_t^{bd} + a_t^{bg} \leq \psi^d. \tag{2.9}$$

The equation (2.4) is for fully satisfying the demand; (2.5) and (2.6) are storage capacity constraints; (2.7) represents that the maximum amount of energy used from wind is bounded by W_t; and finally, (2.8) and (2.9) constrain the decisions to within the storage transfer rates.

Let η=(0, 0, -1, ϕ^c, ϕ^c, -ϕ^d) be a vector containing the flow coefficients for a decision a_t with respect to the storage device. Then, the transition function can be written as,

$$B_{t+1} = B_t + a_t \eta^T. \tag{2.10}$$

The contribution function $R(S_t, a_t)$ is the revenue of the system from being in the state S_t and making the decision a_t at time t as,

$$R(S_t, a_t) = P_t(D_t + \phi^d a_t^{bg} - a_t^{gb} - a_t^{gd}). \tag{2.11}$$

2.2.2 Energy Storage Life Loss Cost

The life loss level of batteries can be measured by using the effective cumulative *Ah* throughput as [18],

$$L_{loss} = \frac{A_c}{A_{total}}. \tag{2.12}$$

where, L_{loss} is the life loss of batteries that depends on both state variable (S_t) and decision vector (a_t), A_c is the effective cumulative *Ah* throughput in a certain period of time. A_{total} is the total cumulative *Ah* throughput in life cycle. A lead-acid battery size of QAh will deliver $390Q$ effective *Ah* over its lifetime [66].

The operational strategy of the system for controlling energy storage life loss cost is illustrated in Figure 2.2. According to Figure 2.2, if battery *SOC* is less than the SOC_{min} then energy is brought from the power grid to fulfill the demand as well as to charge the battery with subject to equations (2.4) to (2.9). Again if battery *SOC* is greater than the set-up *SOC* (SOC_{stp}) then the energy transferred from the battery to demand and to grid subject to equations (2.4) to (2.9).

The effective cumulative *Ah* throughput A_c depends on the operating *SOC* and the actual *Ah* throughput $A_c^{'}$. It can be expressed as,

$$A_c = \lambda_{soc} A_c'. \tag{2.13}$$

where λ_{soc} is the effective weighting factor. In this chapter, the lower limit of the battery *SOC* (SOC_{min}) is set to 0.5 and when *SOC* is greater than 0.5, the effective weighting

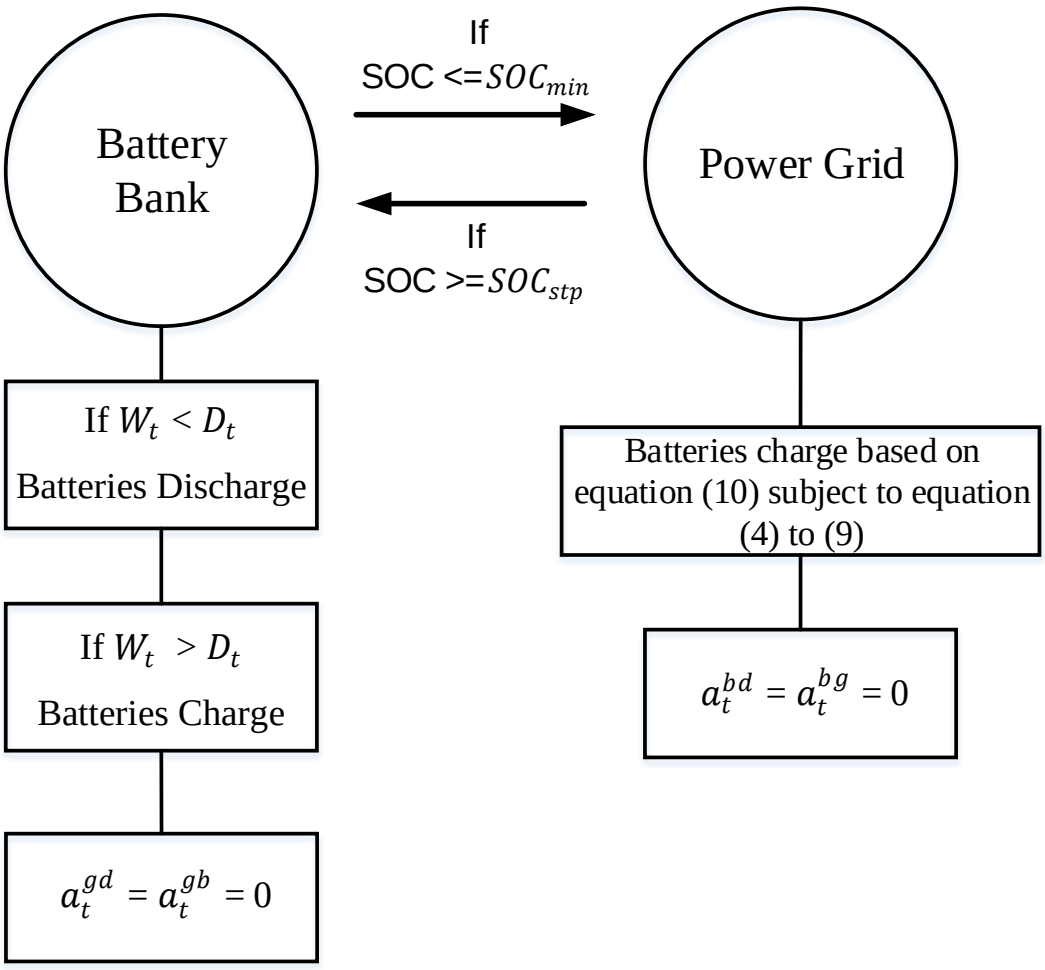

Figure 2.2. Schematic diagram of the energy storage system operation strategy.

factor is approximately linear with *SOC*, which can be expressed as,

$$\lambda_{soc} = m * SOC + n. \tag{2.14}$$

In the equation, *m* and *n* are the two empirical parameters and their values can be determined from Figure 2.3.

The actual *Ah* throughput $A_c^{'}$ is the sum of total energy discharge from the battery at any given time 't' as,

$$A_c^{'} = a_t^{bd} + a_t^{bg} \tag{2.15}$$

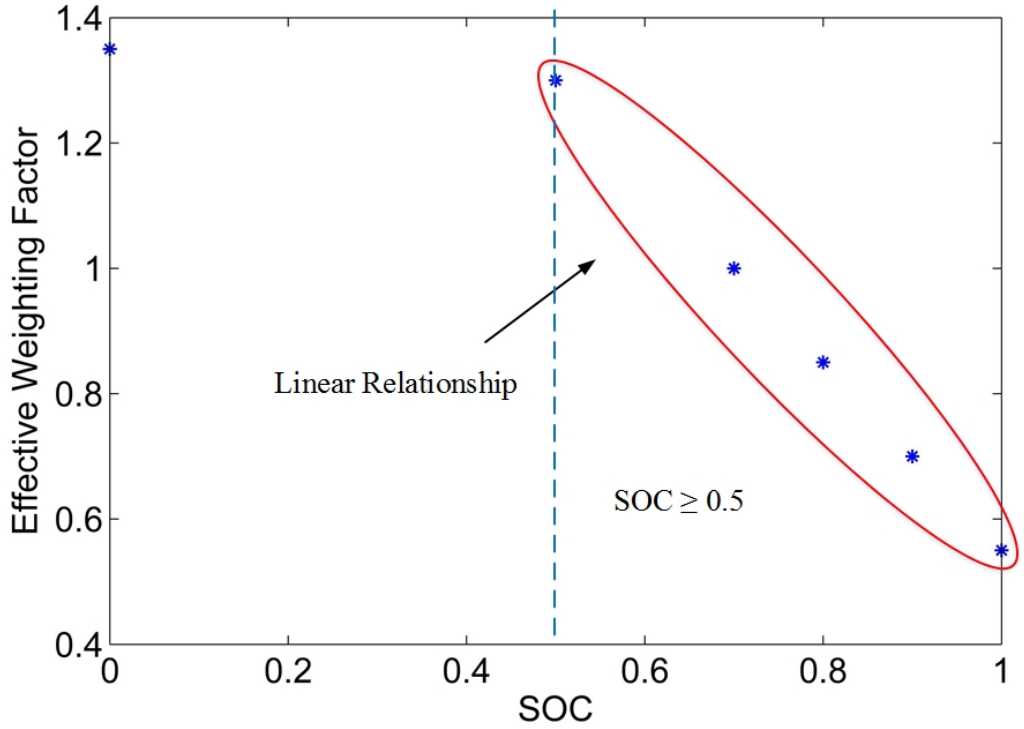

Figure 2.3. Relationship between effective weighting factor and the SOC of lead-acid battery.

Figure 2.3 shows the relation between the operating *SOC* values and the effective cumulative lifetime for lead-acid battery. For instance, when battery *SOC* is 0.5, removing 1 Ah from the battery is equivalent to removing 1.3 Ah from the total cumulative lifetime. However, when battery *SOC* is 0.5, removing 1 Ah from the battery will result in only 0.55 Ah being removed from the total cumulative lifetime. This relation shows that the lead-acid batteries should be operated at high *SOC* to increase their lifetime.

Finally, the life loss cost C_{bl} for a certain duration can be written as,

$$C_{bl} = L_{loss} I_{init-bat}. \tag{2.16}$$

where, $I_{init-bat}$ is the initial investment cost of batteries which is assumed as $\$30,000$.

2.2.3 Objective Function

In this chapter, the main objective is to maximize the total profit over time with the consideration of battery life loss cost. Both equation (2.11) and (2.16) are used to obtain the net revenue of the system at time t as,

$$R_{net}(S_t, a_t) = \max_{a_t \in \chi_t} [R(S_t, a_t) - C_{bl}]. \tag{2.17}$$

The goal is to maximize the total system revenue as well as to minimize the battery life loss cost. The optimal control policy of ADP is used to select an action that will maximize the system revenue and minimize battery life loss cost. The total system revenue function over a finite horizon of time can be expressed as,

$$V = \max_{a_t \in \chi_t} \sum_{t=0}^{T-1} R_{net}(S_t, a_t) \tag{2.18}$$

The life loss cost depends on the SOC level of the battery. To minimize the battery life loss cost, the SOC of the battery needs to set up as high as possible.

2.3 Algorithm Designs

2.3.1 Dynamic Programming Design

In terms of revenue, the optimal solution of stochastic problems can be obtained for problems that have denumerable and relatively small state (S_t), decision (χ_t) and outcome

spaces (W_t). In these case, Bellman's optimality equation can be expressed as,

$$V_t^*(S_t) = \max_{a_t \in \chi_t} [R_{net}(S_t, a_t) + \sum_{s'=1}^{|S_t|} P_t(s'|S_t, a_t) V_{t+\Delta t}^*(s')], \tag{2.19}$$

where, $P_t(s'|S_t, a_t)$ is the conditional transition probability of going from state S_t to state s' for the decision a_t, and where $V_{T+\Delta t}^* = 0$. After solving (2.19), the model can be simulated as a MDP by following the optimal policy, π^*, that is defined by the optimal value functions $(V_t^*)_{t\varepsilon\tau}$.

The MDP can be simulated for a given sample path ω by solving the decision as,

$$X_t^\pi(S_t(\omega)) = arg \max_{a_t \in \chi_t} [R_{net}(S_t(\omega), a_t) + \sum_{s'=1}^{|S_t(\omega)|} P_t(s'|S_t(\omega), a_t) \upsilon], \tag{2.20}$$

where, $\upsilon = V_{t+\Delta t}^*(s'|S_t(\omega), a_t)$ and $S_{t+1}(\omega) = S^M(S_t(\omega), X_t^\pi(S_t(\omega)), W_{t+1}(\omega))$.

For stochastic transition from S_t to s', a statistical estimate of the value of the optimal policy can be calculated as,

$$\overline{V} = \frac{1}{K} \sum_{k=1}^{K} \sum_{t\varepsilon\tau} R_{net}(S_t(\omega^k), X_t^\pi(S_t(\omega^k))). \tag{2.21}$$

where, K = 256 different sample paths, $\{\omega^1, ..., \omega^K\}$.

The effective cumulative Ah throughput in a certain period of time A_c is simulated for K different sample paths, $\{\omega^1, ..., \omega^K\}$ and then a statistical estimate of battery life loss is obtained as,

$$\bar{L}_{loss} = \frac{\frac{1}{K} \sum_{k=1}^{K} \sum_{t\varepsilon\tau} A_c(\omega^k)}{A_{total}}. \tag{2.22}$$

Then, the battery life loss cost is calculated using equation (2.16).

2.3.2 Proposed Adaptive Dynamic Programming Design

The revenue that is obtained at time t can be expressed as Bellman's optimality equation by using the available information of contribution/ revenue function in section 2.2 as,

$$V_t^*(S_t) = \max_{a_t \in \chi_t} [R_{net}(S_t, a_t) + E(V_{t+1}^*(S_{t+1})|S_t)]. \tag{2.23}$$

where S_{t+1} depends on both states (S_t) and a_t. Moreover, the boundary conditions are $R_T^*(S_T) = 0$ and $t \leq T$.

It is often troublesome to deal with an expectation operator due to the high dimension of the state space. Here, post-decision formulation of Bellman's equation is used to overcome this problem as,

$$V_t^*(S_t) = \max_{a_t \in \chi_t} [R_{net}(S_t, a_t) + V_t^a(S_t^a)]. \tag{2.24}$$

where, the expectation operator $E(V_{t+1}^*(S_{t+1}|S_t)$ is replaced by the post-decision value function $V_t^a(S_t^a)$. The post-decision state S_t^a is the state instantly after the current decision a_t is made, but before the arrival of any new information [41].

For calculating battery life loss, the actual Ah throughput $A_c^{'}$ is obtained from the status of the state variable B_t in equation 3.1 for each period of time. During simulation, battery SOC is kept in a certain range and the effective weighting factor is determined from Fig. Then the battery life is calculated as,

$$L_{loss} = \frac{\frac{1}{I}\sum_{i=1}^{I}\sum_{t\varepsilon\tau} A_c}{A_{total}}. \tag{2.25}$$

where, i is the number of iterations and I is the maximum number of iterations. Then equation (2.16) is used to get the battery life loss cost.

In this chapter, ADP is presented as a version of approximate value iteration (AVI). The main advantage of ADP is the rate of convergence [67]. By taking advantage of AVI, ADP can solve optimal benchmark problems within a relatively small number of iterations.

Table 2.1. The Proposed Algorithm

Step 0.

a. Initialize $V_t^{a,0}(s) = 0$ for each $s \varepsilon S$, and $t \leq T-1$.

b. Set $V_T^{a,n}(s) = 0$ for each $s \varepsilon S$, and $n \leq N$.

c. Set n=1.

d. Initialize S_0^1.

Step 1. Choose a sample path ω^n.

Step 2. For $t \leq (T-1)$:

a. Solve:

$$\hat{v_t}^n = \min_{a_t \in \chi_t} [R_{net}(S_t^n, a_t) + V_t^{a,n-1}(S^{M,a}(S_t^n, a_t))].$$

b. If $t > 0$, update $V_{t-1}^{a,n-1}$ using,

$$V_{t-1}^{a,n}(S_{t-1}^{a,n}) = (1-\alpha_{n-1}) V_{t-1}^{a,n-1}(S_{t-1}^{a,n}) + \alpha_{n-1} \hat{v_t}^n.$$

c. Find the post-decision state:

$$S_t^{a,n} = S^{M,a}(S_t^n, a_t^n).$$

d. The next pre-decision state:

$$S_{t+1}^n = S^M(S_t^n, a_t^n, E_{t+1}(\omega^n)).$$

Step 3. If $n < N$, increment n and return **Step 1.**

The proposed algorithm is presented in Table 2.1. Initially, a suitable value function approximation $V_t^a(S_t^a)$ is assumed. Then, n numbers of sample paths are chosen in $step$ 1. In $step$ $2a$, the value of being in state S_t^n is calculated and the post-decision value function approximation is updated in $step$ $2b$. In $step$ $2b$, α_{n-1} is known as a "stepsize", and generally takes on values between 0 and 1. It is often defined as "smoothing", a "linear

filter" or "stochastic approximation". The post-decision state is figured out in $step\ 2c$ and the next pre-decision state is found in $step\ 2d$. Finally, in $step\ 3$, if the number of iteration is less than the maximum number of iteration, the n is incremented and the system is returned to $step\ 1$.

2.4 Simulation Setup and Results Analysis

2.4.1 Simulation Setup

In this section, the numerical simulation results are shown for maximizing net system revenue. The optimal benchmark problem is presented for stochastic time-dependent problems for single energy storage system in the presence of exogenous information such as wind, prices, and demand. The objective function is validated for several stochastic benchmark problems to test the sensitivity of the ADP algorithm to the BESS parameters in the allocation of storage energy. The system is also tested by setting different battery *SOC* level to analyze how battery *SOC* affects the net system revenue. The system is also validated for real-time market price. The lead acid battery parameters are presented in Table 2.2.

Table 2.2. Battery Parameters

Battery	Lead-Acid
Type	2V/1000 Ah
Capacity	30 MWh
Cycle Life	1000 @ 50% DOD
Charging and Discharging Efficiencies (ϕ^c and ϕ^d)	80%
Charging and Discharging Rates (ψ^c and ψ^d)	8 MWh/Δt

The other major parameters like maximum and minimum values of wind energy, load demand, and grid price are summarized in Table 2.3.

Table 2.3. The System Parameters

Name	Wind Energy (MWh)	Load Demand (MWh)	Grid Price ($/MWh)
Maximum value	7	7	70
Minimum value	1	1	30

The stochastic load demand is assumed as that in [68],

$$D_{t+1} = min\{max\{D_t + \Phi^D_{t+1}, D_{min}\}, D_{max}\} \tag{2.26}$$

where, Φ^D_{t+1} is pseudonormally $N(0, 2^2)$ discretized over $\{0, \pm 1, \pm 2\}$, in order to model the seasonality that often remains in observed energy demand. And, the load demand D_t is assumed as,

$$D_t = \lfloor 3 - 4sin(2\pi(t+1)/T) \rfloor \tag{2.27}$$

where, $\lfloor . \rfloor$ represents the floor function.

The first-order Markov chain is investigated to model the stochastic wind power supply and w^W_t i.i.d random variables that can be either uniformly or pseudonormally distributed as,

$$W_{t+1} = min\{max\{W_t + w_{t+1}, W_{min}\}, W_{max}\} \tag{2.28}$$

For the grid price process P_t, three types of stochastic processes are tested, they are 1st-order Markov chain, 1st-order Markov chain plus jump, and sinusoidal. Similar to wind process, p^P_t random variables can be either uniformly or pseudonormally distributed as,

$$P_{t+1} = min\{max\{P_t + p_{t+1}, P_{min}\}, P_{max}\} \tag{2.29}$$

Simulation results are presented in following subsections. All the simulations are conducted in *MATLAB* 2014*a* environment.

2.4.2 Stochastic Experiment Study

The complex stochastic benchmark problems for validating the system are presented in Table 2.4. In Table 2.4, for wind energy and grid price, two different probability distribution functions are used where U and N functions are defined as uniform and pseudonormal distribution respectively. These two probability distribution functions are acted as a noise to make the system stochastic [45]. For all test problems, SOC_{stp} is kept the same as 0.5. The statistical estimate of dynamic programming is treated as optimal value of the system and compared with the proposed ADP. The percentage of optimality of the proposed algorithm is calculated as,

$$\%\ of\ optimality = \frac{V^{1000}}{\overline{V}} \times 100\% \tag{2.30}$$

where, the objective value given by the algorithm after 1000 iterations, V^{1000}, is compared to the statistically estimated optimal value given by DP, $\overline{V}$ in equation (2.21).

Table 2.4. Stochastic Test Problems

No.	W.E.	Price Process	p_t^P
1	$U(-1,1)$	$1stMC + Jump$	$N(0,5.0^2)$
2	$U(-1,1)$	$1stMC + Jump$	$N(0,1.0^2)$
3	$N(0,1.0^2)$	$1stMC + Jump$	$N(0,5.0^2)$
4	$N(0,3.0^2)$	$1stMC + Jump$	$N(0,2.5^2)$
5	$N(0,0.5^2)$	$1st - MC$	$N(0,1.0^2)$
6	$N(0,1.0^2)$	$1st - MC$	$N(0,1.0^2)$
7	$N(0,0.5^2)$	$1st - MC$	$N(0,5.0^2)$
8	$U(-1,1)$	*Sinusoidal*	$N(0,25.0^2)$
9	$N(0,0.5^2)$	*Sinusoidal*	$N(0,25.0^2)$
10	$N(0,1.0^2)$	*Sinusoidal*	$N(0,25.0^2)$

The stochastic benchmark problems in Table 2.4 are used to compare our results with DP. The results are shown in Table 3.4. For example, in test problem 4 from Table 2.4, the pseudonormal probability distribution is used for both stochastic wind energy and grid price. According to Table 2.5, the net total system revenue for problem 4 is found as $ 3793.37 where the optimal value is obtained from DP as $ 3855.44 and then the percentage of optimality is calculated as 98.39 % which is very promising. The other results are also showed that the ADP can obtain at least 98% of optimality for the stochastic case study that proves that the ADP can be a powerful tool of solving optimal policies for stochastic environments.

Table 2.5. Results for Stochastic Test Problems.

No.	R ($)	C_{bl} ($)	R_{net} ($)	Optimal Value ($)	% of opt (%)
1	4191.16	277.67	3913.49	3973.49	98.49 %
2	4188.36	302.78	3885.58	3916.52	99.21 %
3	3987.98	377.49	3610.49	3624.63	99.61 %
4	4192.31	398.94	3793.37	3855.44	98.39 %
5	4211.03	412.29	3798.74	3804.83	99.84 %
6	4038.44	321.68	3716.76	3761.52	98.81 %
7	4169.87	372.29	3797.58	3832.07	99.10 %
8	4218.64	414.06	3804.58	3842.23	99.02 %
9	4029.72	318.53	3711.19	3731.34	99.46 %
10	4174.53	376.34	3798.19	3814.21	99.58 %

2.4.3 Stochastic Experiment Study with Different Battery SOC Setup

The stochastic test problem No. 4 of Table 2.4 is used for more analysis to see the effect of Battery *SOC* on the total system revenue. The results are presented in Table 3.5. The experiment is conducted for four different SOC_{stp} where the SOC_{stp} is varied form 0.55 to 0.63. According to the Table 3.5, the higher and lower system revenues are obtained at 0.55 and 0.63 respectively. The other results show that higher SOC_{stp} of the

battery may cause lower revenue of the system. However, the life loss cost of the battery decreases with the increase of battery *SOC*. As battery life loss cost is proportional to battery lifetime, sacrificing a small amount of revenue may increase battery lifetime as well as the consistency of the system.

In this experiment study, the performance of the proposed ADP approach is also validated for different SOC_{stp} and the results show that the solution of ADP is very close to the optimal solution of DP. The percentage of optimality results are presented in Table 2.6.

Table 2.6. Percentage of Optimality for Stochastic Problem 4 with Different SOC_{stp}.

No.	SOC_{stp}	R ($)	C_{bl} ($)	R_{net} ($)	OV ($)	% of opt. (%)
1	0.55	4058.12	316.92	3741.20	3793.55	98.62%
2	0.58	3971.08	265.31	3705.77	3736.79	99.17%
3	0.60	3906.57	237.48	3669.09	3695.69	99.28%
4	0.63	3806.40	202.73	3603.67	3645.96	98.84%

2.4.4 Experiment Study with Real-time pricing

Table 2.7. Results of the total revenue calculation for real-time pricing.

No.	SOC_{stp}	R ($)	C_{bl} ($)	R_{net} ($)
1	0.55	2249.81	234.03	2015.78
2	0.60	2198.20	218.62	1979.58
3	0.63	2163.11	210.23	1952.88
4	0.65	2138.67	204.95	1933.72

For further analysis, real-time market price is used where the wind energy output is obtained using 1^{st} order Markov chain. For real-time market price, the price data of April 1, 2016 is used [69]. The wind energy output, load demand and grid price are presented in Figure 2.4. The wind energy output signal is obtained using the stochastic test problem 6. Like Table 3.5, battery *SOC* analysis is also conducted with this setup. The results are summarized in Table 2.7.

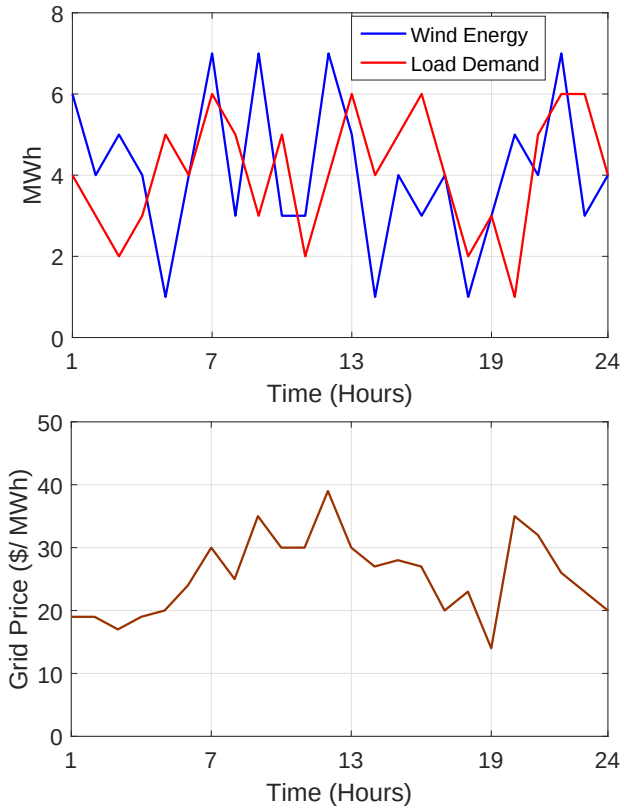

Figure 2.4. Available wind energy, load demand and grid price for April 1, 2016.

In Table 2.7, the results are obtained for four different SOC_{stp} where the values are 0.55, 0.60, 0.63 and 0.65 respectively. According to the results, it is clear that the system revenue has an inversely proportional relationship with battery *SOC*. Higher SOC_{stp} of the battery can provide batteries a better condition to effectively reduce the battery life loss as well as increase the battery lifetime. The system operation profile for problem no. 2 of Table 2.7 is presented in Figure 2.5 where SOC_{stp} is set to 0.6. The three different colors green, blue, and red represent the amount of energy transferring from battery to grid, battery to load demand and grid to battery respectively. The wind energy is dedicated to fulfill the load demand and after fulfilling the demand, the rest of the energy goes to charge the battery if needed. The grid energy is also available to supply the energy to the system when needed.

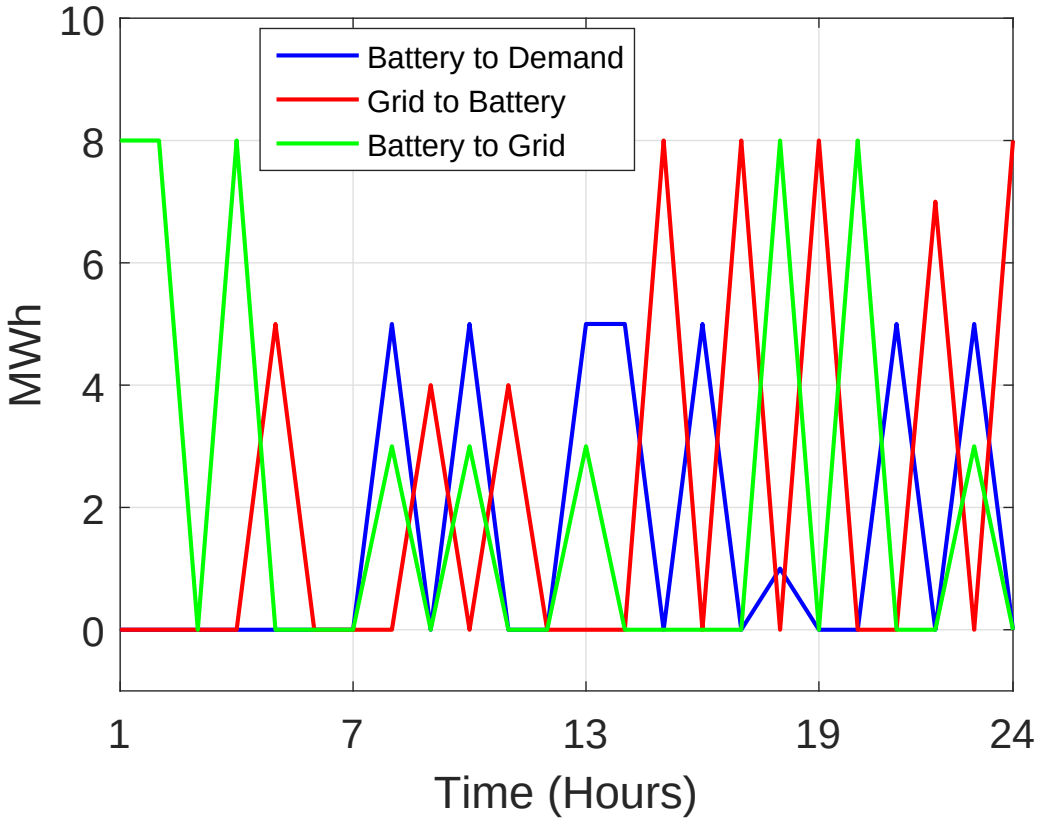

Figure 2.5. System operation profile under the operation strategy of No.2 from Table 2.7.

The *SOC* status of the battery is shown in Figure 2.6. From Figure 2.6, it is clear that whenever battery *SOC* goes below the SOC_{min} level, the control policy of ADP charge the battery from the grid up to the operator defined SOC_{stp} level. In general case, the system has the tendency to discharge the battery at its maximum discharging rate to maximize the system revenue. However, when battery *SOC* is reached at equal or lower state of SOC_{stp}, the system is stopped selling energy to the grid to keep the battery *SOC* close to SOC_{min} to maintain the healthy operation of battery. In some critical situations like time period 14, the load demand, the available wind energy and the battery *SOC* were 4 MWh, 1 MWh and 0.53 respectively. In this situation, the control policy has no way to fulfill the demand without compromising the healthy operation of BESS. In this case, the

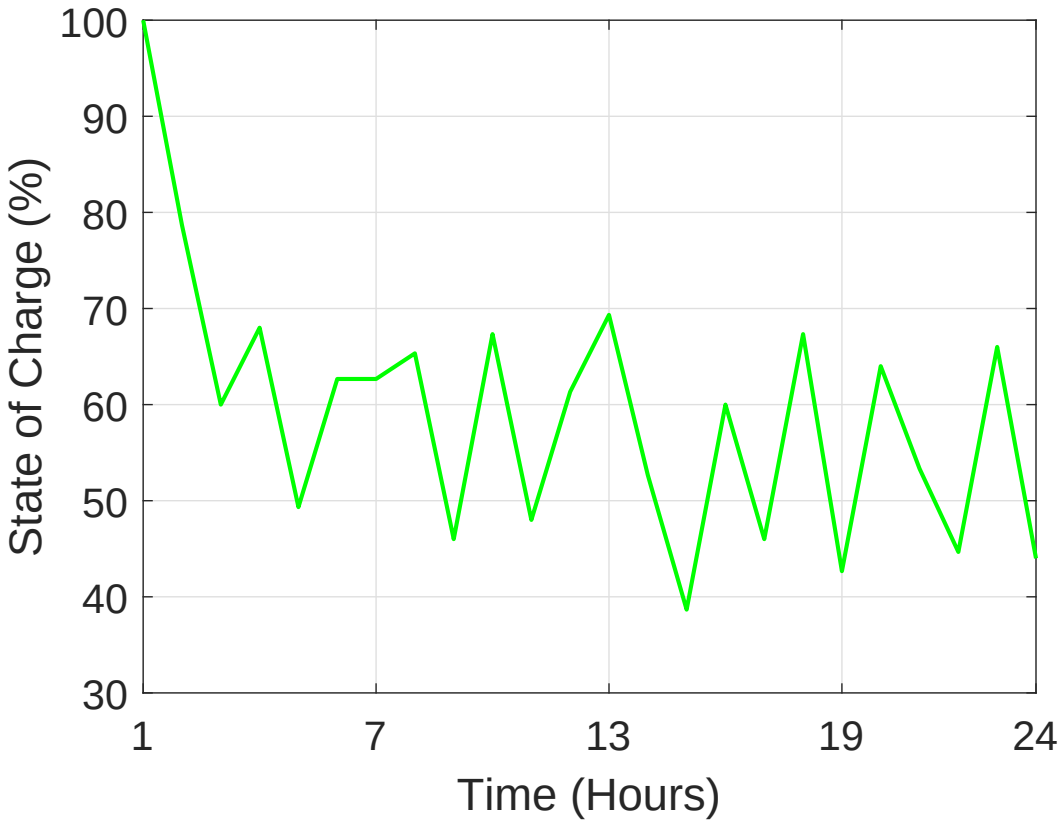

Figure 2.6. Battery SOC changing over time under the operation strategy of No.2 from Table 2.7.

system has transferred energy from the BESS to fulfill the load demand and stopped selling energy to the grid. When the system has more than enough energy after fulfilling the demand, that storage energy is used to sell to the grid to get the revenue. However, if the storage does not have enough energy to get charged from the wind energy, the system buys that energy from the grid to keep battery *SOC* above the defined level as well as to reduce battery life loss cost.

2.5 Summary

In this chapter, near optimal operation of energy storage system is discussed with the presence of wind energy, load demand and power grid by considering lifetime

characteristics. The problem is formulated as a MDP, and the near optimal policy is simulated by proposed ADP. To verify the performance of the proposed algorithm, DP is used to statistically estimate the optimal value of the total system revenue and compared with the proposed ADP approach. The proposed ADP approach successfully approximated the solution that was very close to the optimal solution of DP. Simulation studies have been carried out for three cases: ten different stochastic test problems were investigated and validated with DP, one stochastic test problem is used by varying battery SOC_{stp} to see the effect of battery SOC on the total system revenue and for further analysis real-time pricing is also used. The simulation results show that ADP is a powerful tool for the power system optimization problem that can provide sequential optimal decision and control to address optimal operation of BESS.

CHAPTER 3 Computationally Efficient Optimization for Islanded Microgrid

3.1 Nomenclature

B_t : Amount of energy in the storage device at time t, in kWh.

W_t : Net amount of output power of wind turbine available at time t, in kW.

D_t : Aggregate power load demand at time t, in kW.

a_t^{wd} : Amount of power transferring from wind turbine to demand, in kW.

a_t^{gd} : Amount of power transferring from diesel generator to demand, in kW.

a_t^{bd} : Amount of power transferring from battery to demand, in kW.

a_t^{wb} : Amount of power transferring from wind turbine to battery, in kW.

a_t^{gb} : Amount of power transferring from diesel generator to demand, in kW.

χ_t : Feasible action space.

B^c : Energy capacity of the storage device, in kWh.

ϕ^c : Charging efficiency of the device.

ϕ^d : Discharging efficiency of the device.

ψ^c : Maximum charging rates of the device, in $kWh/\Delta t$.

ψ^d : Maximum discharging rates of the device, in $kWh/\Delta t$.

B_{min} : Minimum limit of the storage device, in kWh.

υ_i : Cut-in speed for wind turbine, in m/s.

υ_o : Cut-off speed for wind turbine, in m/s.

υ_r : Rated wind speed, in m/s.

W_r : Rated output power of the wind turbine, in kW.

SOC_{max} : Upper limit of battery state of charge.

SOC_{min} : Lower limit of battery state of charge.

C_w : Battery wear cost, in $\$/kWh$.

P_t^B : Total amount of energy discharge from the BESS at time t, in kWh.

λ_{soc} : Effective weighting factor that depends on the battery SOC for each time period.

p and q : Two empirical parameters.

C_i : Initial investment cost for BESS, in \$.

δ : Depth of discharge (DOD) of BESS.

N_c : Corresponding number of life cycle at rated DOD.

P_{rated} : Rated output power of the diesel generator, in kW.

P_{gen} : Actual output power of the diesel generator, in kW.

L_0 and L_1 : Fuel consumption curve fitting coefficients.

F : Fuel price for diesel generator, in $\$/L$.

C_{die-om} : Operation and maintenance cost of the diesel generator, in \$.

$C_{die-loss}$: Diesel generator life loss cost, in \$.

E_t : Vector which contains exogenous information.

w_{t+1} : Change in the renewable energy at time $t+1$.

d_{t+1} : Change in the demand at time $t+1$.

G_t : Available power capacity of the diesel generator, in kW.

M_1 and M_2 : Weights.

K : Number of different sample paths, $\{\omega^1, ..., \omega^K\}$.

α_{n-1} : Step-size for n-th iteration.

$\hat{V}$: Estimated value obtained from the proposed ADP approach after given iterations.

V^* : Optimal value obtained from the DP (for stochastic cases) or LP (for deterministic cases).

3.2 Introduction

Basically, in the islanded microgrid, the power generation capacity are limited. The distributed energy sources are the key power resources in islanded microgrid, especially in remote areas. In islanded microgrid, the uncertain behavior of the DERs presents many challenges in power generation and load balance maintenance to ensure power network stability and reliability. Also, in islanded microgrids, it is a challenge to optimize the BESSs with other power supply units (e.g., DERs and traditional power generator) and

achieve the minimum daily operational cost. Also, in the islanded microgrid, it is uneconomical to replace the BESS frequently due to transportation and labor cost. So, it is often desired to control and coordinate the BESS in an efficient and economical way. In this chapter, the optimal operation of the BESSs in the islanded microgrid is investigated by considering battery lifetime characteristics where The battery parameters, which have significant effects on the battery lifetime like maximum charging and discharging rate, maximum charging and discharging efficiency and maximum capacity, are also taken into account. Compared to prior works (e.g., [45], [70], [68], [71]) the main contributions of this paper are as follows:

- A new energy optimization problem for islanded microgrid is formulated as a MDP, where the wind energy, the BESS, and the diesel generator models are taken into consideration. A proper control strategy for *SOC* is also developed for the healthy operation of the BESS. Different from the other prior works, the proposed model considers the operation of the islanded microgrid, and the uncertainty of wind energy and the battery lifetime characteristics are included.

- An efficient ADP approach is proposed to solve the energy optimization problem formulated above on both deterministic and stochastic cases. ADP can achieve the same optimality performance as that of LP in deterministic cases [72], and competitive optimality performance as that of DP for stochastic cases. The computational time of ADP approach is around 50% less that of DP. Yearly simulation results using ADP approach provide the net savings for different *SOC*s, yet the traditional DP is not feasible to solve it.

- The performance of ADP approach is also justified using large data samples and compared with the traditional DP approach. The result shows that the ADP approach can achieve near optimal operation on average 9.29 times faster response than the traditional DP approach for different stochastic test problems with 0.2 million of data samples. To further validate the performance of the proposed ADP, different sets of data samples are used for each time instance and found that the proposed ADP approach can achieve approximately 18.69 times faster response than the traditional DP approach in seconds for 0.5 million of data samples.

3.3 Model Description of Islanded Microgrid

The structure of the island microgrid is illustrated in Figure 3.1. The system is configured with a wind turbine, a battery bank, and a diesel generator as power supply units as well as load demands as power demand units. The diesel generator serves as the backup power source in case of emergency. In the model, the wind turbine and diesel generator units are responsible to charge the battery when the SOC of the battery goes below a certain limit. The charge controller (CC) is used to prevent over-charging of the battery. The dumping load is used to absorb the excessive energy produced by supply units of the system. The problem of allocating BESS energy is considered over a finite horizon of time as $\tau = \{0, \Delta t, 2\Delta t, ..., T - \Delta t, T - 1\}$, where $\Delta t = 1$ hour is the time step and $T = 25$ hours.

The state variable of the system at any time instance t can be written as,

$$S_t = (B_t, W_t, D_t). \tag{3.1}$$

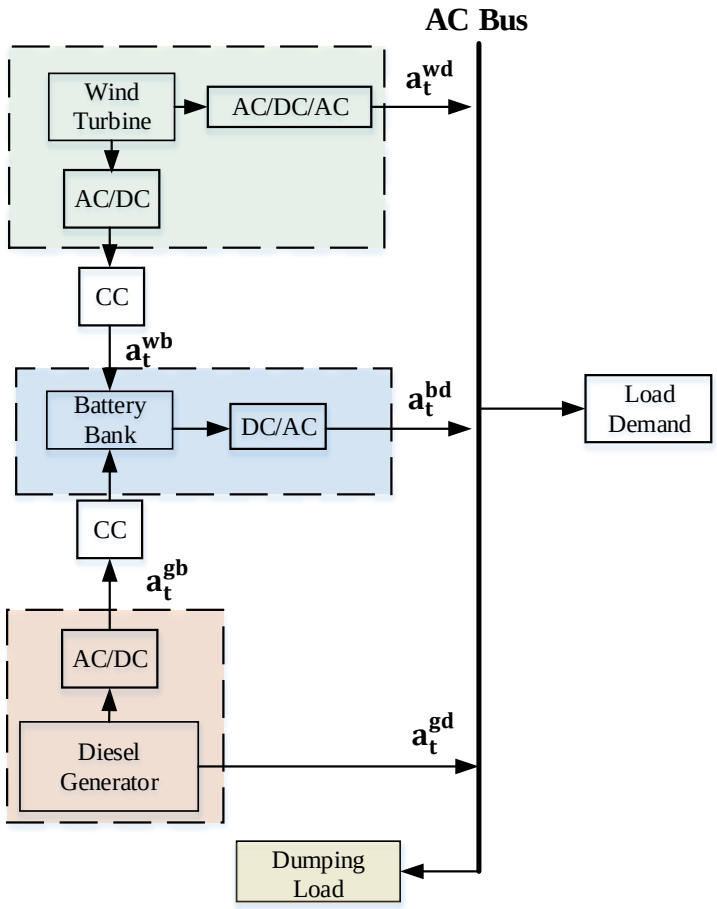

Figure 3.1. The power system model diagram for an islanded microgrid, where the arrows represent the transferred power among dash blocks. The AC/DC or DC/AC blocks are representing the converters which are required to transfer power from one system to another.

In the model, the transferring power from one unit (dash block) to another unit is defined as action. There are five different actions in the model, and these allocation actions are defined by the five-dimensional, nonnegative decision vector as,

$$a_t = (a_t^{wd}, a_t^{gd}, a_t^{bd}, a_t^{wb}, a_t^{gb})^{\tau} \geq 0, a_t \in \chi_t, t \in \tau. \tag{3.2}$$

where, a_t^{ij} means power transferred from i to j at time t. The superscript w, d, g and b

represents wind, demand, generator and battery, respectively. In equation (3.2), each variable represents the amount of transferring power from one unit to another unit. For an example, a_t^{wd} is representing a certain amount of power from the wind turbine to the load demand based on the operational constraints.

3.4 Problem Formulation

3.4.1 Wind Power Generation Model

The wind turbine is one of the major power supply units of the islanded microgrid which is integrated into the system as a renewable source. The wind power output can be related to wind speed approximately by using the following function as [18],

$$W_t = \begin{cases} 0 & v < v_i \; or \; v > v_o \\ \frac{W_r(v-v_i)}{(v_r-v_i)} & v_i \leq v \leq v_r \\ W_r & v_r \leq v \leq v_o \end{cases}$$

3.4.2 BESS Model

The BESS is one of the core parts of the island microgrid system. The strategy of optimizing the BESS significantly impacts the performance of the overall system.

For the healthy operation of BESS, the SOC of the BESS should be within a certain range as,

$$SOC_{min} \leq SOC \leq SOC_{max} \tag{3.3}$$

The next-hour *SOC* of the BESS can be determined by the *SOC* value at time t and the battery power during the time period. The equation for determining the next hour *SOC*

can be expressed as,

$$SOC_{t+\Delta t} = SOC_t + soc_t. \tag{3.4}$$

The soc_t can be defined as,

$$soc_t = \frac{\phi^c (a_t^{gb} + a_t^{wb})}{B^c} - \frac{a_t^{bd}}{B^c \phi^d}. \tag{3.5}$$

where, the battery's mode of operation can be determined by the value of soc_t. The battery's charging, discharging and standby modes can be defined by the positive, negative and zero numbers of soc_t value, respectively.

The daily operational cost function for BESS can be written as,

$$C_t^{BESS} = C_w P_t^B \Delta t. \tag{3.6}$$

For each time instance t, the discharging energy from the BESS can be calculated as,

$$P_t^B = a_t^{bd} \lambda_{soc}. \tag{3.7}$$

In this chapter, SOC_{min} is set to 0.5 and when SOC is greater than 0.5, the effective weighting factor is approximately linear with SOC, which can be expressed as [71], [66],

$$\lambda_{soc} = p * SOC + q. \tag{3.8}$$

λ_{soc} is the effective weighting factor that depends on the battery SOC for each time period.

According to the existing papers [18], [71] and [66], when the battery *SOC* is higher than 0.5, the effective weighting factor is approximately linear with *SOC*. For instance, for a lead-acid battery, when battery *SOC* is 0.5, removing 1 Ah from the battery is equivalent to removing 1.3 Ah from the total cumulative lifetime. So, the effective weighting factor is 1.3. However, when battery *SOC* is 1, removing 1 Ah from the battery will result in only 0.55 Ah being removed from the total cumulative lifetime, so in this case, the effective weighting factor is 0.55.

The battery wear cost function can be expressed as,

$$C_w = \frac{C_i}{\phi^d B^c N_c \delta}. \tag{3.9}$$

In the equation of the battery wear cost, the initial investment cost for the battery (C_i), in \$, is used as the numerator and the expected battery lifetime, in kWh, is used as the denominator. In this chapter, the battery wear cost is representing the cost in \$ per kWh of the battery.

3.4.3 Diesel Generator Daily Operational Cost Model

Diesel generators generally serve as a backup power source. The fuel consumption (L) of the diesel generators is modeled as a linear function of their actual output power as,

$$L_t = (L_0 \times P_{rated} + L_1 \times P_t^{gen}). \tag{3.10}$$

Based on the recommended value from [73], L_0 and L_1 are set as 0.08415 and 0.246 respectively. The actual output power of the diesel generator, P_t^{gen}, can be calculated as,

$$P_t^{gen} = a_t^{gd} + a_t^{gb}. \tag{3.11}$$

Diesel generators usually have power limits which can be expressed as,

$$k_{gen} P_{rated} \leq P_t^{gen} \leq P_{rated}. \tag{3.12}$$

where, the value of k_{gen} is set to 0.3 based on the manufacturer's suggestion [18].

The daily operational of diesel generator can be calculated as,

$$C_t^{gen} = C_t^{die-fuel} + C_{die-om} + C_{die-loss}. \tag{3.13}$$

where, $C_t^{die-fuel}$ is the fuel cost of the diesel generator that can be expressed as,

$$C_t^{die-fuel} = F \times L_t. \tag{3.14}$$

3.4.4 Transition Function for Exogenous Information and Constraints

For exogenous information, let E_t= (W_t,D_t) and S_t = (B_t,E_t), where E_t is independent of B_t. Next if the exogenous information, e_{t+1}, to be the change in E_t as,

$$E_{t+1} = E_t + e_{t+1}. \tag{3.15}$$

where, between time t and $t+1$, $e_{t+1} = (w_{t+1}, d_{t+1})$; The exogenous information e_{t+1} is independent of S_t and a_t.

The set of constraints are as follows,

$$a_t^{wd} + a_t^{gd} + a_t^{bd} = D_t. \tag{3.16}$$

$$a_t^{wb} + a_t^{wd} \leq W_t. \tag{3.17}$$

$$a_t^{wb} + a_t^{gb} \leq min(\frac{B^c - B_t}{\Delta t}, \psi^c). \tag{3.18}$$

$$a_t^{gb} + a_t^{gd} \leq G_t. \tag{3.19}$$

$$a_t^{bd} \leq min(\frac{B_t - B_{min}}{\Delta t}, \psi^d). \tag{3.20}$$

The available power capacity of the diesel generator G_t depends on the fuel availability. In this chapter, it is considered that enough fuel is available to satisfy the load demand and to charge the BESS.

A battery control strategy is illustrated in Figure 3.2. A controllable parameter set-up state of charge (SOC_{stp}) is introduced in Figure 3.2 which is defined by the operator. The value of SOC_{stp} should be higher than the SOC_{min} of the battery. In every time step, the system compares the battery SOC with the defined SOC_{stp} and find out the multiple number of combinations of decision vectors which decision vectors obey the constraints according to the control policy. Later, a decision vector is selected which minimized the operational cost of the system. At the beginning of the operation strategy, the system

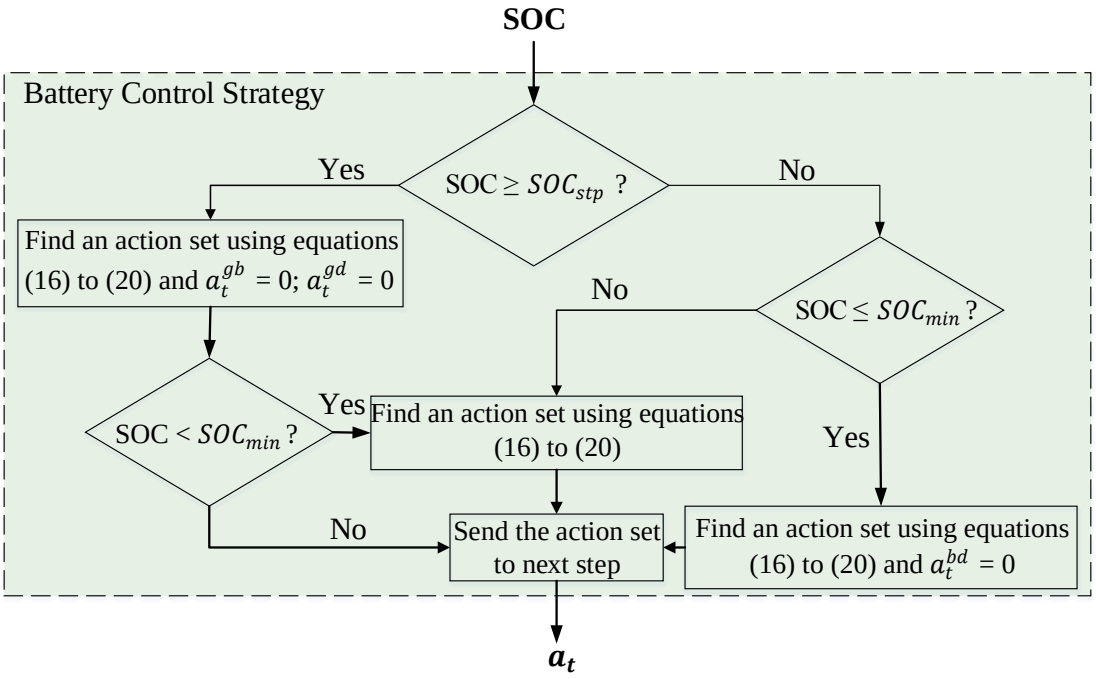

Figure 3.2. The proposed battery control strategy algorithm for battery SOC.

checks the SOC condition of the battery. If it is higher than the defined SOC_{stp}, then the decisions of the diesel generator a_t^{gd} and a_t^{gb}, are assumed as 0. Then the next-hour battery *SOC* is calculated. If the next-hour SOC is less than the SOC_{min}, the system decides to keep the constraints unchanged instead of defining generator decisions a_t^{gd} and a_t^{gb} as 0 and then go to the next step. If the battery *SOC* is less than the defined SOC_{stp}, the system compares battery *SOC* with SOC_{min}. At this step, if the system finds the battery *SOC* less or equal to the SOC_{min}, then the system is added one constraint to make battery action a_t^{bd} as 0, otherwise it decides to keep the constraints unchanged instead of defining battery decision a_t^{bd} as 0 and then go to the next step. This process of selection of the battery operation strategy continues over the finite horizon of time until $t = T - 1$.

3.4.5 Objective Function

A weighted sum method is used for the objective function where the daily operational cost of diesel generator and BESS are combined with two weights. The goal of this objective cost function is to minimize total cost of operation in islanded microgrid. The cost function can be written as,

$$C(S_t, a_t) = M_1 \times C_t^{gen} + M_2 \times C_t^{BESS}. \tag{3.21}$$

where, the weights M_1 and M_2 are determined by the priority of each objective. For example, if $M_1 = M_2 = 0.5$ then two objectives are treated as equally important. If one weight is greater than the other one, it indicates that the objective with the higher weight is more important to achieve the overall goal.

The total system objective function over a finite horizon of time can be expressed as,

$$V = \min_{a_t \in \chi_t} \mathbb{E}[\sum_{t=0}^{T-1} C(S_t, a_t)]. \tag{3.22}$$

where, $\mathbb{E}[.]$ is the expectation operator. For stochastic case study, two stochastic variables are considered, and they are wind power output and load demand. The stochastic equations for stochastic variables are presented in section 3.6.1 and the probability distribution functions are summarized in section 3.6.3. The expectation operator is not used for the deterministic case study.

The overall goal is to find a proper set of actions

$$a_t = arg \min_{a_t \in \chi_t} V. \tag{3.23}$$

such that the total system objective function V can be minimized over time.

3.5 Algorithm Designs

3.5.1 Linear Programming Design

LP is a technique used for optimization that takes various linear inequalities relating to some situation, and finds the optimal solution under those conditions [72]. If the state variables are deterministic and the dynamics are known a *priori*, the problem can be solved by the LP. Based on the set of constraints that are presented in section III, the problem can be formulated as a LP problem over the defined time horizon as,

$$V^* = \min \sum_{t=0}^{T-1} C(S_t, a_t) \tag{3.24}$$

Subject to,

$$AX \leq B \tag{3.25}$$

$$A_{eq}X = B_{eq} \tag{3.26}$$

where, the objective is to minimize the total cost function over time that is defined in equation 3.24. A and B are the inequity constraint parameters, A_{eq} and B_{eq} are the equality constraint parameters and X is the set of actions that is defined in equation (3.2) in section 3.2. Both inequality and equality constraints are depend on the mode defines in the control strategy.

This process is initialized by training the deterministic datasets to the system. Then

the mode of operation of the battery is selected based on the available information. In the next step, the solution of set of actions are obtained using the LP approach and used that solution to calculate the cost function.

This formulation is most useful when the predictions about the state variables are accurate. It is hard to find the physical processes that are intrinsically stochastic, however the deterministic case study allows to test the ability of the algorithm to learn the solution in the presence of set of constraints as well as the objective function.

3.5.2 Dynamic Programming Design

The optimal solution of stochastic problems for minimizing the daily operating cost can be obtained for problems that have denumerable and relatively small state, decision, and outcome spaces [45]. In this case, Bellman's optimality equation can be expressed as,

$$V_t^*(S_t) = \min_{a_t \in \chi_t} [C(S_t, a_t) + \sum_{s'} P_t(s'|S_t, a_t) V_{t+\Delta t}^*(s')], \tag{3.27}$$

where, $P_t(s'|S_t, a_t)$ is the conditional transition probability of going from state S_t to state s' for the decision a_t, and where $V_{T+\Delta t}^* = 0$. In order to solve the equation (3.27), the model can be simulated as a MDP by following the optimal policy, π^*, that is defined by the optimal value functions $(V_t^*)_{t\varepsilon\tau}$.

The MDP can be simulated for a given sample path ω by solving the decision as,

$$\Pi_t^{\pi^*}(S_t(\omega)) = arg \min_{a_t \in \chi_t} [C(S_t(\omega), a_t) + \sum_{s'} P_t(s'|S_t(\omega), a_t) \upsilon], \tag{3.28}$$

where, $\upsilon = V_{t+\Delta t}^*(s'|S_t(\omega), a_t)$ and $S_{t+1}(\omega) = S^M(S_t(\omega), \Pi_t^{\pi^*}(S_t(\omega)), W_{t+1}(\omega))$. Here, $S^M(.)$ is defined as system model which describes how a system evolves from S_t to $S_{t+\Delta t}$ using action a_t and new information $E_{t+\Delta t}$ as, $S_{t+\Delta t} = S^M(S_t, a_t, E_{t+\Delta t})$.

For stochastic transition from S_t to $s^{'}$, a statistical estimated value of the optimal policy can be calculated as,

$$V^* = \frac{1}{K}\sum_{k=1}^{K}\sum_{t\varepsilon\tau} C(S_t(\omega^k), \Pi_t^{\pi^*}(S_t(\omega^k))). \tag{3.29}$$

In this chapter, we use this statistical estimated value as our expected value function.

3.5.3 Proposed Approximate Dynamic Programming Design

The equation (3.27) can be written as an expectation form of Bellman's equation as,

$$V_t^*(S_t) = \min_{a_t\in\chi_t}[C(S_t,a_t) + \mathbb{E}\{V_{t+1}^*(S_{t+1})|S_t\}]. \tag{3.30}$$

where, it is clear that S_{t+1} depends on both S_t and a_t. As in this chapter, the state, action and information spaces are all continuous and multi-dimensional, for simulation and computational purposes, it is usually troublesome to solve this optimization program efficiently with traditional DP approaches [42], [44]. To overcome the curse of dimensionality, a post-decision formulation of Bellman's equation is formulated as,

$$V_t^*(S_t) = \min_{a_t\in\chi_t}[C(S_t,a_t) + V_t^a(S_t^a)]. \tag{3.31}$$

where, the post-decision state S_t^a is the state instantly after the current decision a_t is made, but before the arrival of any new information. An example of state transition is presented in Figure 3.3, where the information available at a decision node (squares) is the pre-decision state, and the information available at an outcome node (circles) is the

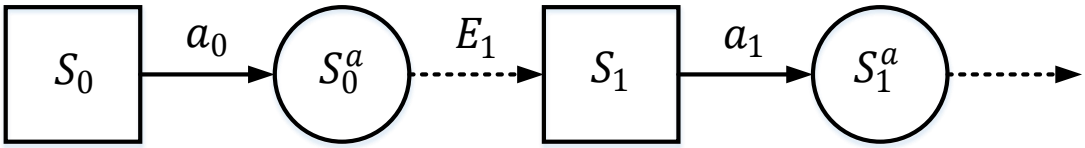

Figure 3.3. The diagram of a state transition, showing decision nodes (squares) and outcome nodes (circles). Solid lines are decisions, and dotted lines are possible outcomes.

post-decision state. The function $S^{M,a}(S_t, a_t)$ takes the system from a decision node to an outcome node and the function $S^{M,W}(S_t^a, W_{t+1})$ takes the system from an outcome node to the next-hour state.

The post-decision value function $V_t^a(S_t^a)$ can be written as,

$$V_t^a(S_t^a) = \mathbb{E}\{V_{t+1}^*(S_{t+1})|S_t^a\}, \tag{3.32}$$

$$V_{t-1}^a(S_{t-1}^a) = \mathbb{E}\{V_t^*(S_t)|S_{t-1}^a\}. \tag{3.33}$$

For any time instance t and number of iteration n, a sample realization of the value of being in the state S_t^n, can be expressed as,

$$\hat{v_t}^n = \min_{a_t \in \chi_t} [C(S_t^n, a_t) + V_t^{a,n-1}(S^{M,a}(S_t^n, a_t))]. \tag{3.34}$$

Using $\hat{v_t}^n$, the post-decision value function approximation can be updated as,

$$V_{t-1}^{a,n}(S_{t-1}^{a,n}) = (1-\alpha_{n-1})V_{t-1}^{a,n-1}(S_{t-1}^{a,n}) + \alpha_{n-1}\hat{v_t}^n. \tag{3.35}$$

where α is a step-size to smooth the value function approximation [45].

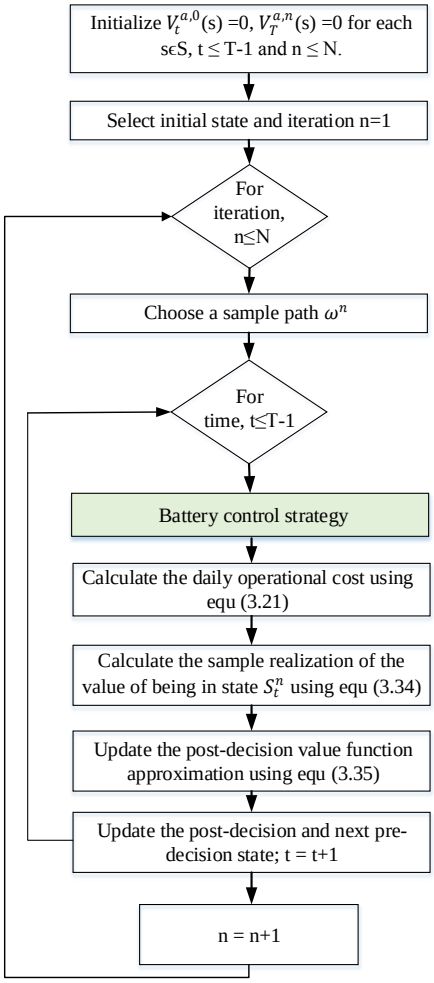

Figure 3.4. The proposed ADP algorithm flow chart.

A complete sketch of the ADP algorithm flow chart using the post-decision state variable is presented in Figure 3.4. In the flow chart, at the beginning, the value functions, number of iteration and state variables are initialized. The iteration begins with choosing a sample path ω^n. Then, the time begins with providing current hour *SOC* information to the battery control strategy algorithm. By training the set of constraints to the system, the proposed control system finds a set of actions that minimize the cost function. In next two steps, the daily operational cost of the microgrid and the sample realization of the value

function are calculated using equations (3.21) and (3.34), respectively. Then, the post-decision value function approximation is updated. In next step, the post-decision and next-hour pre-decision states are updated. At last, the number of iteration n is updated and if $n \leq N$, then the system goes for next iteration.

3.6 Simulation Setup and Results Analysis

3.6.1 Simulation Setup

The BESS parameters are presented in Table 3.1. The other major parameters like maximum and minimum values of wind power, load demand, and power generation of diesel generator are summarized in Table 3.2.

Table 3.1. Battery Parameters

Battery	Lead-Acid
Type	2V/1000 Ah
Quantity	75
Capacity	150 kWh
Minimum limit	75 kWh
Cycle life	1000 @ 50% DOD
Charging and discharging efficiencies (ϕ^c and ϕ^d)	80%
Maximum charging and discharging rates (ψ^c and ψ^d)	50 kWh/Δt
Battery cost	\$80 per kWh
Installation cost	\$20 per kWh
Transportation cost	\$20 per kWh

Table 3.2. The System Parameters

Name	Wind speed (m/s)	Demand (kW)	Diesel generator (kW)	Wind power (kW)
Maximum	30	50	70	50
Minimum	0	20	21	0

For stochastic analysis, to make the system stochastic, different processes are investigated where the random variables are introduced to create noise that can be either

uniformly or pseudonormally distributed.

The stochastic load demand is assumed as,

$$D_{t+1} = min\{max\{D_t + \Phi^D_{t+1}, D_{min}\}, D_{max}\}. \tag{3.36}$$

where, Φ^D_{t+1} is pseudonormally $N(0,2^2)$ discretized over $\{0,\pm1,\pm2\}$, in order to model the seasonality that often remains in observed power demand. Here, $N(0,2^2)$ is representing the pseudonormal probability distribution where the mean value is as 0 and the variance is as 2. To introduce noise into the system, a vector of discrete values from -2 to 2 is used with the interval of 1. The probabilities are calculated for each value in the vector based on the pseudonormal probability density function as that of [45]. Then the next-hour load demand is calculated using the equation (3.36).

The first-order Markov chain is investigated to model the stochastic wind power supply and w^W_t i.i.d random variables that can be either uniformly or pseudonormally distributed as,

$$W_{t+1} = min\{max\{W_t + w_{t+1}, W_{min}\}, W_{max}\}. \tag{3.37}$$

To quantify the percentage of optimality of our proposed algorithm, the percentage of optimality (%) is calculated as,

$$\%\ of\ optimality = \frac{\hat{V}}{V^*} \times 100\%. \tag{3.38}$$

Simulation results are presented in the rest of these sections. All the simulations are conducted in *MATLAB* 2015*b* environment. To conduct the simulations, a computer with

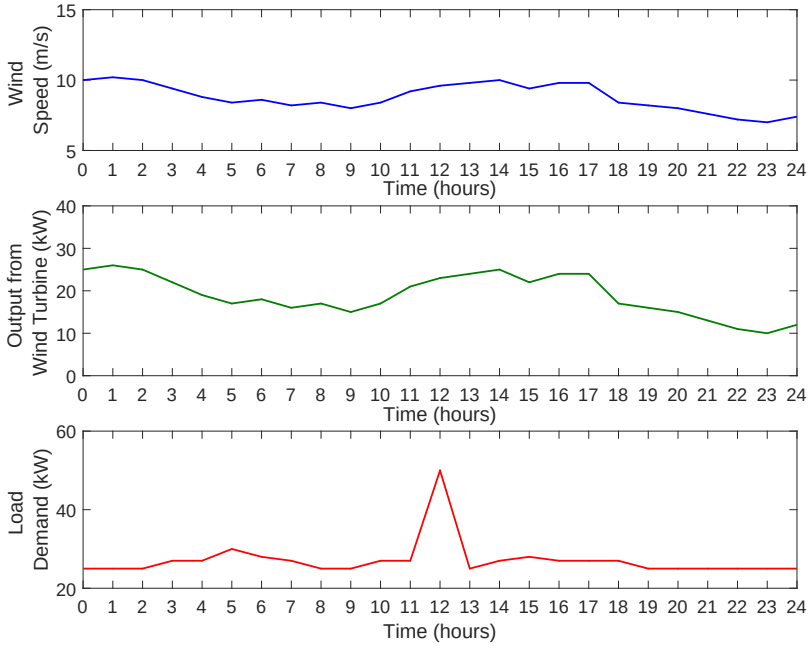

Figure 3.5. Wind speed profile, wind power output and a typical load demand of the island.

3.60 GHz *Intel Core i*7 – 4790 *CPU* processor and 8 *GB RAM* is used.

3.6.2 Deterministic Case Study

Deterministic case study is one of the widely used experiments that is useful to test the optimality of the algorithm. In this section, for the deterministic case study, the system is trained by the deterministic dataset of the wind speed and the load demand. For the experiment, the load demand of the microgrid is considered as 20 kW as average load, whereas the peak load demand is 50 kW. For the wind turbine, the cut-in, cut-off, and rated wind speed are assumed as 5 m/s, 30 m/s, and 15 m/s, respectively. The wind speed is assumed as Figure 3.5. The wind power output is obtained via the model given in Section 3.4. The load demand and the wind power outputs are also presented in Figure 3.5.

The experiment is conducted for different SOC_{stp} environments, where the SOC_{stp} is varied from 0.55 to 0.65. In this experiment, the two weight factors are kept as

Table 3.3. Percentage of Optimality for Deterministic Case with Different SOC_{stp}.

No.	SOC_{stp}	C^{gen} ($)	C^{BESS} ($)	$\hat{V}$ ($)	V^* ($)	% of opt. (%)
1	0.55	185.21	53.16	119.19	119.19	100%
2	0.58	185.21	48.87	117.04	117.04	100%
3	0.60	182.01	44.76	113.39	113.39	100%
4	0.63	182.01	38.34	110.18	110.18	100%
5	0.65	182.01	36.90	109.46	109.46	100%

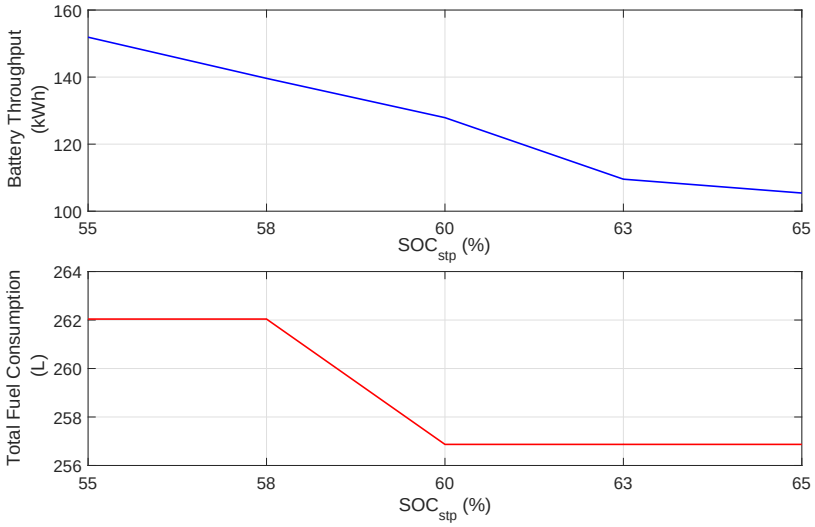

Figure 3.6. The total kWh battery throughput and the total fuel consumption of the diesel generator by varying SOC_{stp}.

$w_1 = w_2 = 0.5$ to treat both objectives equally. The results are summarized in Table 3.3. The estimated value ($\hat{V}$) of ADP is also compared with the expected V^* from the traditional LP. For all cases, the percentage of optimality is obtained as 100%. According to Table 3.3, the daily operational cost of the battery as well as the daily operational cost of the system is decreasing over the increase of SOC_{stp}. The total kWh battery throughput and the total fuel consumption of the diesel generator by varying the SOC_{stp} are shown in Figure 3.6. According to the figure, the total kWh battery throughput is decreasing with the increase of the SOC_{stp}. The total fuel consumption of the diesel generator is found constant as 262.04 L from the SOC_{stp} as 0.55 to 0.58 and as 256.87 L from the SOC_{stp} as

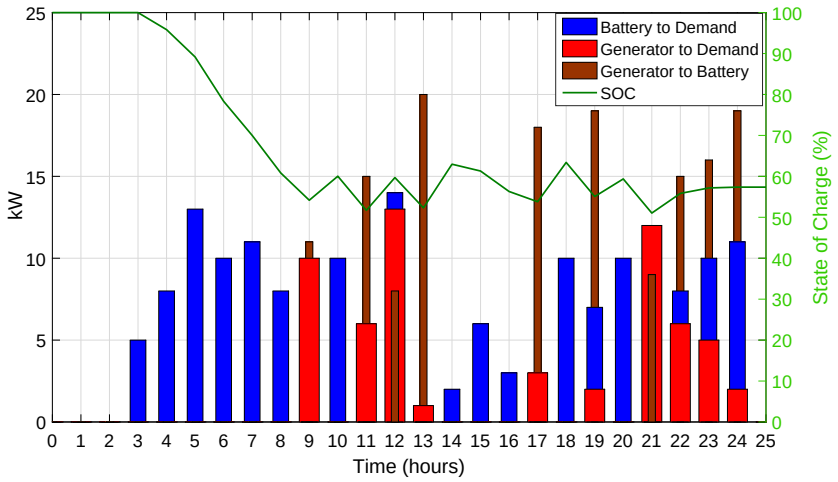

Figure 3.7. The system operation profile under the operation strategy of No.1 in Table 3.3.

0.60 to 0.65.

For the operation scheme of No.1, where the SOC_{stp} is set to 0.55, the system operation profile is presented in Figure 3.7. In Figure 3.7, the blue, red, and brown color bars are representing the transferred energy from the battery to the load demand, the diesel generator to the load demand, and the diesel generator to the battery, respectively. The battery *SOC* curve is also shown in Figure 3.7 in order to show how the system is working. According to the figure, when battery *SOC* stays above the SOC_{stp}, only the battery and the wind power work to fulfill the load demand, and when the battery *SOC* reaches in between SOC_{stp} and SOC_{min}, both the battery and the diesel generator supply power to support the load demand. And when the battery *SOC* reaches at SOC_{min} or below, only the diesel generator supplies the power to the load demand to make the system stable, as well as to charge the battery with its maximum charging limit.

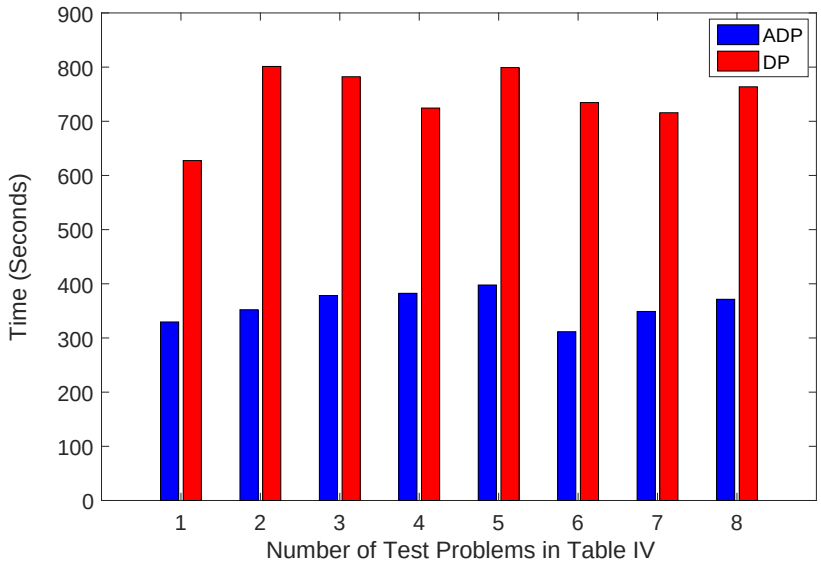

Figure 3.8. The computational time comparison between the DP and ADP.

3.6.3 Stochastic Case Study

The stochastic benchmark problems for validating the system are presented in the second column of Table 3.4. The two different probability distribution functions are used where U and N functions are defined as uniform and pseudonormal distribution, respectively. These two probability distribution functions are used to find the next-hour wind power and load demand [45]. For all test problems, SOC_{stp} is kept the same as 0.6.

Table 3.4. Results for Stochastic Test Problems.

No.	w_t^W	C^{gen} ($)	C^{BESS} ($)	$\hat{V}$ ($)	V^* ($)	% of opt. (%)
1	$U(-1,1)$	162.58	18.45	90.52	91.79	98.62 %
2	$N(0,1.0^2)$	158.36	14.01	86.19	87.93	98.02 %
3	$N(0,3.0^2)$	165.75	20.47	93.11	94.88	98.13 %
4	$N(0,0.5^2)$	164.38	21.06	92.72	93.50	99.17 %
5	$N(0,2.5^2)$	159.06	15.85	87.46	88.64	98.66 %
6	$N(0,1.5^2)$	161.14	21.53	91.34	92.22	99.05 %
7	$N(0,3.5^2)$	163.30	20.82	92.06	93.59	98.37 %
8	$N(0,4^2)$	165.46	21.58	93.52	94.99	98.45 %

Table 3.5. Percentage of Optimality for Stochastic Problem 4 with Different SOC_{stp}.

No.	SOC_{stp}	C^{gen} ($)	C^{BESS} ($)	$\hat{V}$ ($)	V^* ($)	% of opt. (%)
1	0.55	159.89	22.45	91.17	92.72	98.33%
2	0.58	162.57	21.64	92.11	93.72	98.28%
3	0.60	164.38	21.06	92.72	93.50	99.17%
4	0.63	166.82	20.17	93.50	94.81	98.62%

Table 3.6. Yearly Simulation Results for Stochastic Problem No. 4 with Different SOC_{stp}.

No.	SOC_{stp}	Fuel consumption (L)	Weighted battery throughput (kWh)	Weighted total cost of operation ($)	Maximum battery life (years)
1	0.55	93,072.02	21,739.13	36,642.47	2.76
2	0.58	102,004.42	17,804.15	38,722.89	3.37
3	0.60	105,605.49	15,957.45	39,516.06	3.76
4	0.63	108,144.41	14,117.65	39,981.16	4.25

The stochastic benchmark problems in column No.2 of Table 3.4 are used to compare our results with DP. The results are also shown in Table 3.4. According to Table 3.4, the daily operational cost of the system for problem 4 is found as $92.72, where the optimal value is obtained from DP as $93.50, and then the percentage of optimality is calculated as 99.17% which is promising. The other results also show that the ADP can obtain at least 98% of optimality for stochastic case study. The computational time comparisons between the DP and ADP approach are also illustrated in Figure 3.8. For instance, to solve problem No. 4, the computational time cost for the ADP and the DP are found as 382.44 seconds and 724.41 seconds, respectively. In Figure 3.8, the other results show that, the proposed ADP approach takes almost 50% less computational time to solve the problem than the DP approach. The results prove that the ADP can be a powerful tool of solving optimal policies for stochastic environments.

In order to justify the effect of battery *SOC* on the daily operational cost function, the stochastic test problem No. 4 of Table 3.4 is used for more analysis. The results are

presented in Table 3.5. The stochastic test problem is conducted for four different SOC_{stp}. The results show that higher SOC_{stp} of the battery causes lower daily operational cost of the battery. However, the daily operational cost of the diesel generator increases when the battery SOC_{stp} increases. As the daily kWh throughput of the battery is proportional to battery lifetime, sacrificing small amounts of the daily operational cost of the system may increase battery lifetime as well as the consistency of the system.

Moreover, in order to justify the long-term benefits of choosing proper SOC parameters, the yearly simulations are conducted for different SOC_{stp} setups on problem No. 4 from Table 3.4. The results are summarized in Table 3.6. According to Table 3.6, it is noticed that fuel consumption is decreasing with the increase of SOC_{stp} and vice versa for weighted battery throughput. In Table 3.6, the minimum battery lifetime and maximum battery lifetime are found for SOC_{stp} as 0.55 and 0.63, respectively. The warranty of the lead-acid battery is assumed as five years and the total initial investment for battery as $(150kWh \times 120\$/kWh) = \$18,000$. The calculated cost per year for the BESS is $\$3,600$. By changing SOC_{stp} from 0.55 to 0.63, the total cost of operation increases by $\$3,338.69$; however, the battery lifetime increases by 1.49 years, which saves $\$5,364$. So, the estimated net saving of the system can be calculated as $\$5,364 - \$3,338.69 = \$2,025.31$. From the results, it can be concluded that sacrificing small amounts of daily operational cost of the system causes big savings in the future as well as the battery lifetime increment.

3.6.4 Stochastic Case Study for Large Number of Data Samples

For this case study, the stochastic test problems of Table 3.4 are investigated. Since, the performance of the proposed ADP approach in terms of percentage of optimality is

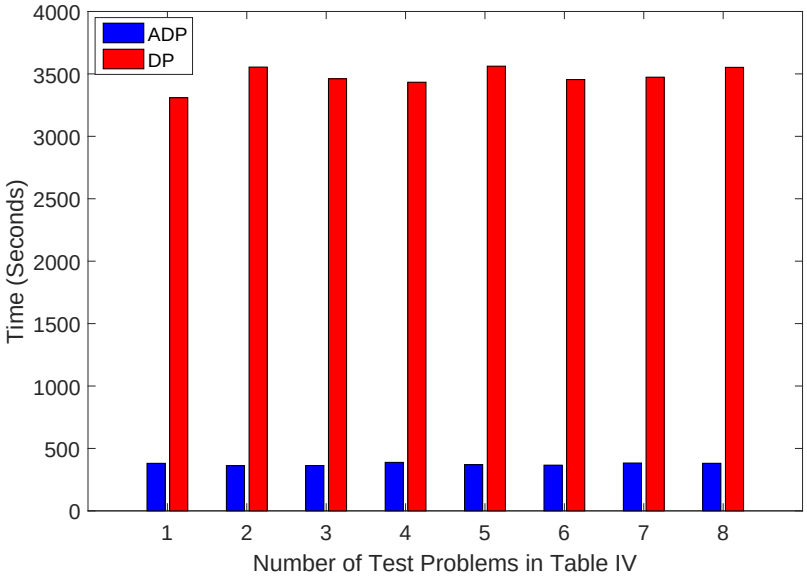

Figure 3.9. The computational time comparison between the traditional DP and the proposed ADP approaches for large data samples.

reported in section 3.6.3, in this section, the performance of the proposed ADP approach in terms of computational time is taken under consideration. The computational time comparisons between the DP and ADP approach for large number of data samples are presented in Figure 3.9 where 0.2 million of data samples are taken into consideration for each time step. The results showed that the proposed ADP performed very well in terms of computational time and achieved on average 9.29 times faster response than the traditional DP approach.

To further validate the performance of the proposed ADP, different sets of data samples are used for each time instance. For this study, the stochastic test problem No. 2 of Table 3.4 is used. The results are illustrated in Figure 3.10. In the figure, the x-axis is representing the number of data samples generated at each time interval where k is representing thousands. According to the results, the computational time for the proposed ADP approach is very low compared to the traditional DP approach. For example, the

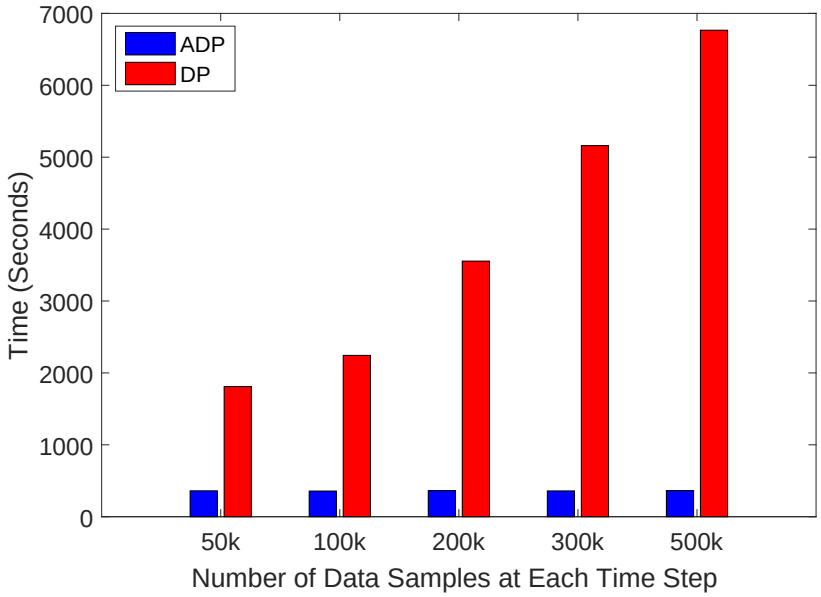

Figure 3.10. The computational time comparison between the traditional DP and the proposed ADP approaches for large data samples.

computational time of the proposed ADP and the traditional DP approach for 0.5 million of data samples is found as 372.01 seconds and 6952.87 seconds, respectively. It shows that the proposed ADP approach achieved approximately 18.69 times faster response than the traditional DP approach for 0.5 million of data samples. Also, the computational time of the proposed ADP approach doesn't change much with the increasing number of data samples. However, the time cost of the traditional DP approach is increasing with the increasing number of data samples. According to the results, it can be concluded that the proposed ADP approach outperformed the traditional DP approach with the increasing number of data samples.

3.7 Summary

In this chapter, the optimal operation of energy systems in an islanded microgrid is investigated considering battery lifetime characteristics. Extensive simulations were

conducted to validate the effectiveness of the proposed ADP approach. The traditional LP and DP were used for the deterministic and stochastic case study, respectively. Simulation results showed that the ADP can achieve 100% for deterministic case study and at least 98% of optimality for stochastic case study with lower computational time, respectively. The computational time comparison was also reported in the simulation results section. Yearly simulation results were presented to estimate the net savings of the system for different *SOC* setups in the control strategy. Moreover, the proposed ADP approach is validated for different data samples. The results showed that the proposed ADP approach outperformed the traditional DP approach with the increasing number of data samples. According to the results, the proposed ADP approach is a computationally efficient tool for the power system optimization problems.

CHAPTER 4 Energy Optimization for Smart Community with Financial Trade-offs

4.1 Nomenclature

N Total number of households.

$P_{AC,i}$ Power rating for the air conditioner of resident i, kW.

$S_{AC,i}$ Status of the air conditioner of resident i.

$To_{Room,i}$ Initial room temperature of resident i, °F.

$LR_{AC,i}$ Room temperature loss rate of resident i.

$TA_{AC,i}$ Ambient temperature for the air conditioner of resident i, °F.

AE_i Effect of the air conditioner of resident i, °F/kW.

$T_{Low,i}$ Low temperature defined by resident i, °F.

$T_{High,i}$ High temperature defined by resident i, °F.

$P_{WH,i}$ Power rating for the electric water heater of resident i, kW.

$S_{WH,i}$ Status of the electric water heater of resident i.

$To_{WH,i}$ Initial tank temperature for the electric water heater resident i, °F.

$T_{WH,L,i}$ Low temperature for the electric water heater defined by resident i, °F.

$T_{WH,H,i}$ High temperature for the electric water heater defined by resident i, °F.

$LR_{WH,i}$ Tank temperature loss rate of resident i.

$TA_{WH,i}$ Ambient temperature for the electric water heater of resident i, °F.

E_i Effect of the electric water heater of resident i, °F/kW.

$P_{h,CD,i}$ Cloth dryer heating rated power of resident i, kW.

$S_{CD,i}$ Control signal from residential energy management system for the cloth dryer of resident i.

$P_{m,CD,i}$ Cloth dryer motor rated power of resident i, kW.

$T_{CD,i}$ Operation status of the clothes dryer of resident i.

$P_{h,DW,i}$ Dish washer heating rated power of resident i, kW.

$S_{DW,i}$ Control signal from residential energy management system for the dish washer of resident i.

$P_{m,DW,i}$ Dish washer motor rated power of resident i, kW.

$T_{DW,i}$ Operation status for the dish washer of resident i.

$P_{EV,i}$ Electric vehicle rated power of resident i, kW.

$S_{EV,i}$ Status of the electric vehicle of resident i.

$p_{cri,i}$ Critical loads of resident i, kW.

TA_i Total number of appliances of resident i.

NA_i Total number of active appliances of resident i.

CP_i User defined number of active appliances should be turned on.

R_1 Level 1 reward rate, $cents/kW.5minutes$.

R_2 Level 2 reward rate, $cents/kW.5minutes$.

R_3 Level 3 reward rate, $cents/kW.5minutes$.

$P_{total,i}$ Power consumption capacity of resident i, kW.

$P_{c,i}$ Total power consumption of resident i, kW.

$P_{L,i}$ Lower bound of the power consumption defined by resident i, kW.

M Large enough constant.

v_i Binary variable.

w Weight of comfort indicator.

a Priority number.

4.2 Introduction

The DSM is one of the widely researched techniques for future smart grid in the field of power system optimization. It receives increasing attention by power research and industry due to its potential to improve the efficiency and quality of the power systems. According to [10], in the U.S.A., residential load demands consume 38% of total electricity energy consumption. Residential demand-side resources have the potential to participate for improving the power system operation. In this chapter, a CEMS is proposed for aggregating residential demands. In the proposed strategy, the CEMS serves as an agent of the utility. The role of the proposed energy optimization scheme is not only

to distribute demand reduction request by the utility among residential appliances quickly and efficiently without affecting residents' comfort levels but also to strategically reward the residents for their participation.

Compared to prior works, instead of considering only thermal-related electric appliances, the proposed energy optimization scheme considers all the residential home electric appliances in demand response and scheduling. It performs an efficient DRR and also maintains the comfort levels for the consumers, in addition to minimize the total reward costs of the utility during peak hours. Specifically, a new comfort indicator is designed to include total power consumption and temperature (e.g., temperature controlled by air conditioners and water heater), and a corresponding reward function is also designed accordingly to satisfy various types of consumers. The problem is then formulated as to minimize the sum of total reward cost for utility and comfort indicator. Note, minimizing comfort indicator is to maximize the comfort level of consumers. The performance of the proposed approach is compared with the existing approaches in [11] and [74] in terms of total rewards for the utility and average comfort level of residents.

4.3 Overview of the Community Energy Management System

The proposed model and information flow chart are illustrated in Figure 4.1. In the proposed design, the CEMS serves as the agent who receives DRRs from the utility and residential load parameters from every household as shown in Figure 4.1. Then, the CEMS generates the optimal control strategy for residential appliances based on user's preferences and send the estimated rewards to the utility.

For the IBDR program participants, the proposed strategy can 1) distribute financial

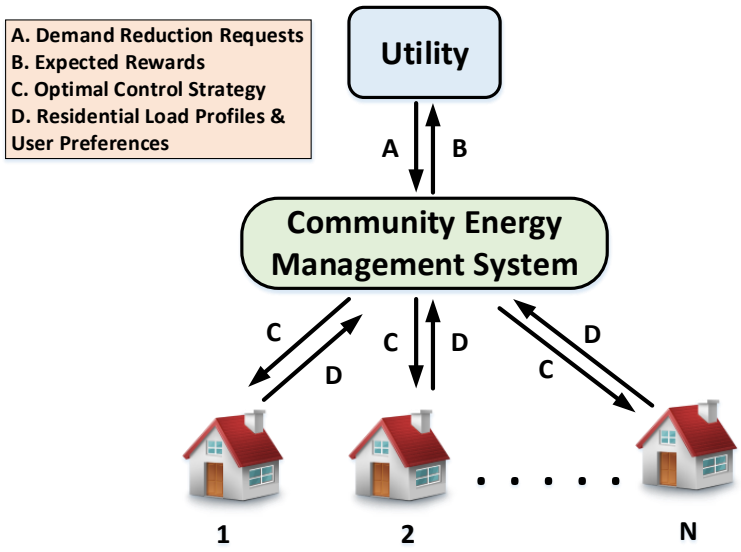

Figure 4.1. The proposed model and information flow.

rewards according to their quantified participations in the DR events, and 2) maintain their comfort level based on their energy consumption preferences. For the utility, the proposed strategy can 1) executed the DRRs by controlling residential appliances, and 2) minimize the total reward costs of the utility for performing DRRs. By benefiting both users and utility, the proposed approach may attract more DR program participants and further utilize the potential capability of controllable residential demand-side resources.

4.4 Residential Appliance Models

Residential appliances can be classified into two types, 1) controllable or non-critical loads, and 2) uncontrollable or critical loads. The controllable loads have high potential to participate in the DR events and to earn rewards. The controllable appliances are controlled by the CEMS and the CEMS is responsible to change the status of the controllable appliances in response to the specified demand limit by the utility.

4.4.1 Air Conditioner Model

Air conditioner (AC) is one the major controllable residential appliances. The power consumption of the AC depends on the operating status of the AC like if the status is ON, it consumes the rated power, and if the status is OFF, then the AC power consumption is zero. The power consumption equation of the AC for resident i can be expressed as [52], [75],

$$p_{AC,i} = P_{AC,i}.S_{AC,i} \tag{4.1}$$

where, $P_{AC,i}$ is the rated power value for the air conditioner of resident i which is different for different houses. $S_{AC,i}$ represents the ON/OFF status where $S_{AC,i} = 1_{\{T_{Room,i} > T_{High,i}\}}$.

The indoor air temperature can be estimated using the ACs as [11],

$$T_{Room,i} = To_{Room,i} - LR_{AC,i}(To_{Room,i} - TA_{AC,i}) + AE_i.p_{AC,i} \tag{4.2}$$

where, the parameters $LR_{RM,i}$, AE_i, and $p_{AC,i}$ are different for each residents.

4.4.2 Electric Water Heater Model

The power consumption of the electric water heater (EWH) can be calculated as [52], [75],

$$p_{WH,i} = P_{WH,i}.S_{WH,i} \tag{4.3}$$

where, the power consumption of the EWH depends on the operating status of the EWH like the AC. $S_{WH,i}$ represents the ON/OFF status where $S_{WH,i} = 1_{\{T_{WH,i} < T_{WH,L,i}\}}$.

For estimating the water temperature in EWH, the equation can be written as [11],

$$T_{WH,i} = To_{WH,i} - LR_{WH,i}(To_{WH,i} - TA_{WH,i}) + E_i.p_{WH,i} \tag{4.4}$$

where, the parameters $LR_{WH,i}$, E_i, and $p_{WH,i}$ are different for each residents.

4.4.3 Cloth Dryer and Dishwasher

The cloth dryer (CD) and dishwasher (DW), both are task based appliances. Usually, in these appliance models, two power consumption parts need to be considered, one is for motor part and another one is for heating coils. The power consumption equation of the cloth dryer can be expressed as [76],

$$p_{CD,i} = P_{h,CD,i}.S_{CD,i} + P_{m,CD}.T_{CD,i} \tag{4.5}$$

Like the CD, the power consumption equation of the dishwasher can be written as,

$$p_{DW,i} = P_{h,DW,i}.S_{DW,i} + P_{m,DW}.T_{DW,i} \tag{4.6}$$

4.4.4 Electric Vehicle Model

The power consumption by the electric vehicle (EV) for charging, can be written as [52], [75],

$$p_{EV,i} = P_{EV,i}.S_{EV,i} \tag{4.7}$$

4.4.5 Critical Loads

The critical loads (CLs) of the household may include refrigeration, freezing, cooking, lighting and other non-controllable electric appliances. A random profile which has a maximum value of 2 kW and a minimum value of 1 kW is selected in the simulation

program [52], [75], [77].

4.5 Energy Optimization Objectives and Solution Designs

4.5.1 Conventional Approach

The adopted conventional approach is illustrated in Figure 4.2 [74], [77]. According to the control strategy, at each time period, whenever total power consumption of the community goes above the demand limit defined by the utility, then DR event starts. The system distributes the DRR to the residents equally. Then, the system calculates the distributed rewards and the total power consumption for each house, and sends the information to the utility. Then the system goes to the next time period and follow the same procedure.

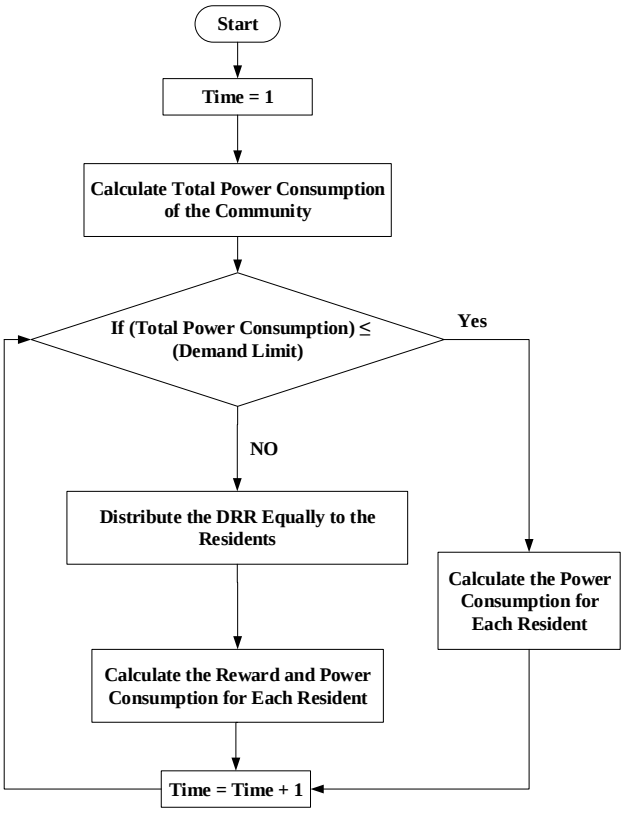

Figure 4.2. Conventional approach for optimizing residential load demand.

4.5.2 Proposed Optimization Strategy

When the utility sends the DRR signal to the CEMS, distributing that DRR to the residents considering their comfort level is the most critical issue for the CEMS. In this work, the proposed approach introduces the concept of a ”Comfort Indicator” to solve this issue. A weighted sum normalized equation is used to define the comfort indicator (CI) where the temperature of the air conditioner and water heater as well as the number of the active appliances are taken under consideration. A normalized equation of the CI considering the temperature of the air conditioner can be expressed as,

$$CI_{AC,i} = \left| \frac{2T_{Room,i} - T_{Low,i} - T_{High,i}}{T_{High,i} - T_{Low,i}} \right| \tag{4.8}$$

The mean value of the user defined high and low bound of the comfort temperature range is assumed to be the ideal operating point. The $CI_{AC,i}$ represents the distance between the current status and the ideal operating point. According to this equation, if the $CI_{AC,i}$ value is getting high, the resident i will start feeling uncomfortable and vice versa. Similarly, the normalized equation of the CI considering the temperature of the water heater can be written as,

$$CI_{WH,i} = \left| \frac{2T_{WH,i} - T_{WH,L,i} - T_{WH,H,i}}{T_{WH,H,i} - T_{WH,L,i}} \right| \tag{4.9}$$

During peak hours, the comfort level of the resident is also depend on the number of appliances he/ she can use. In peak time period, all the users want to best use their appliances, and load curtailment may hamper their daily life. Since, this is also an issue of

the user's comfort level, an appliance status based CI is also introduced as,

$$CI_{S,i} = \left| \frac{TA_i - NA_i}{TA_i - CP_i} \right| \tag{4.10}$$

For resident i, the appliance status set can be expressed as,

$$S_i = \{S_{AC,i}, S_{WH,i}, S_{CD,i}, S_{DW,i}, S_{EV,i}, S_{cri,i}\}. \tag{4.11}$$

where, for counting the number of active appliances NA_i, the status of the AC and WH are assumed as $S_{AC,i} = 1_{\{T_{Room,i} \leq T_{High,i}\}}$ and $S_{WH,i} = 1_{\{T_{WH,i} \geq T_{WH,L,i}\}}$, respectively. The status of all critical loads $S_{cri,i}$ is always 1.

Therefore, the number of active appliances NA_i for resident i can be calculated as,

$$NA_i = \sum_i S_i. \tag{4.12}$$

Considering above three CIs, a weighted sum normalized CI can be written as,

$$CI_i = w_1.CI_{AC,i} + w_2.CI_{WH,i} + w_3.CI_{S,i} \tag{4.13}$$

where, w_1, w_2 and w_3 are the weights.

The relationship between $CI_{i,t}$ and the reward rates can be written as,

$$RWR_{i,t} = \begin{cases} R_1, & if \quad CI_i \leq 1 \\ R_2, & if \quad CI_i > 1 \ \ and \ \ compromise_i = 1 \\ R_3, & if \quad CI_i > 1 \ \ and \ \ compromise_i = 0 \end{cases}$$

According to the strategy, to get the rewards, the resident must needs to be participated. The participant needs to share information of the residential load profile, comfort temperature setting ranges for temperature dependent appliances, priority list of the appliances (if any), and whether he/she is willing to compromise his/her comfort level by curtailing the loads. The lowest and highest rewards are R_1 and R_3, respectively. Any resident may intentionally choose $compromise_i = 0$, to gain more financial benefits with the expectation to receive the highest reward rate, R_3. However, the emergency cases may occur very rarely such that the resident may not have much chance to receive reward at the rate R_3 while losing more probable opportunities to receive rebates at R_2 rate. In any emergency case, to maintain the stability of the power system, the utility may send a DRR with a tremendous amount to the CEMS. Then, the CEMS executes such DRR by curtailing the loads of the resident, who claims not to compromise. In this case, the participant will get the reward at R_3 rate.

According to the equation, if the CI_i value is less than 1, the user will be rewarded at R_1 rate. Again, if the CI_i value is greater than 1 and want to compromise ($compromise_i = 1$), then the user will receive reward at R_2 rate. And R_3 reward is for the users who do not want to compromise ($compromise_i = 0$) and whose CI_i value is greater than 1.

When the CEMS receives a DRR, it should try to maintain a similar comfort margin for each resident in the controlled area while performing the load curtailment. To solve this issue, overall comfort levels have been considered in the objective function of the optimization problem. Also, to be fair for all the residents, the CEMS keeps a record of the DRR participation history for every resident. Whenever the CEMS finds the residents with same CI values, the CEMS will choose the one with a lower DRR contribution history to maintain a fair and equal opportunity for all the residents.

To formulate the optimization problem, the reward rates can be redefined as,

$$RWR_i = R_1.v_i + R_2.(1-v_i).com_i + R_3.(1-v_i).(1-com_i) \tag{4.14}$$

where, v_i is a binary variable [78] and com_i is representing $compromise_i$ which is described in section 4.5.

The objective is to minimize total reward cost for the utility while maximizing the residents' comfort levels (thereby minimizing comfort indictor). The objective function can be expressed as,

$$min\{\sum_{i=1}^{N} RW_i + w.\sum_{i=1}^{N} CI_i\} \tag{4.15}$$

Subject to the constraints as,

$$\sum_{i=1}^{N}(P_{total,i} - P_{c,i}) \geq DRR \tag{4.16}$$

$$P_{L,i} - P_{c,i} \leq M(1-v_i) \tag{4.17}$$

$$P_{L,i} - P_{c,i} > -Mv_i \tag{4.18}$$

$$RW_i = (P_{total,i} - P_{c,i}).RWR_i \tag{4.19}$$

$$P_{c,i} = \sum_{a=1}^{NA_i} P_{con,i} \tag{4.20}$$

where, for resident i, the appliance power consumption set can be expressed as,

$$P_{con,i} = \{p_{AC,i}, p_{WH,i}, p_{CD,i}, p_{DW,i}, p_{EV,i}, p_{cri,i}\}. \tag{4.21}$$

To solve this non-linear optimization problem, genetic algorithm (GA) has been used. The GA is a popular optimization technique that can be used for both linear and non-linear problems for solving both constrained and unconstrained optimization problems. The GA optimizes based on a natural selection process that mimics biological evolution where the algorithm repeatedly modifies a population of individual solutions. The GA selects individuals from the current population randomly at each step and uses them as parents to produce the children for the next generation. In this way, over the successive generations, the population approaches toward an optimal solution.

The proposed optimization scheme flowchart is illustrated in Figure 4.3. At each time step, the system sends residential load profiles and user preferences to the CEMS. Based on the available information, the CEMS optimizes the power consumption for each house. Then, the appliances are turned on based on the user's priority and the optimal power consumption limit. During the optimization, the system also checks the temperature of the AC and EWH for each house. If the temperatures are within the limit, then the CEMS allocate that energy to the next available appliances based on the user's

priority by turning off the AC and EWH. After optimizing the power consumption of each houses, then the system calculates the total financial rewards and the comfort level for each house. Later, the system checks the time step and if it is less then T, then the system goes through the procedure again.

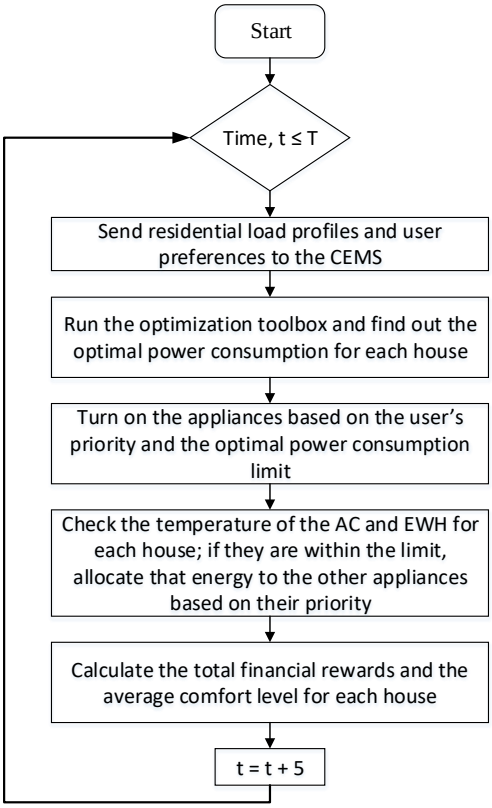

Figure 4.3. The proposed optimization approach for optimizing residential load demands.

4.6 Simulation Setup and Results Analysis

In this section, we have three case studies for 10-house energy optimization experiment and one case study for 100-house energy optimization experiment. All the case studies are compared with existing approaches in terms of reward incentives and comfort levels. A community with ten houses is first considered. In the community, every

resident has different personal preferences and load profiles. Six different appliances are considered where AC, EWH, CD, DW and EV are considered as controllable loads and CLs are considered as non-controllable loads. The power rating of the appliances of each house is presented in Table 4.1 [11], [52], [75], [77]. All the residents might not have all the appliances. In the table, the unavailable appliances are defined as 0. The total power demand of the community is calculated as 136.9 kW.

Table 4.1. Load Profiles for Ten Residents.

House No.	AC (kW)	EWH (kW)	CD (kW)	DW (kW)	EV (kW)	CLs (kW)
1	1.4	4	3.7	3.1	4	1.1
2	1.2	3.9	4	2.9	0	1.3
3	1.5	3.5	4.1	3.2	3.8	1.3
4	1.6	3.8	0	2.8	0	1.1
5	1.3	3.1	3.4	0	3.6	1.4
6	1.2	3.4	3.8	3	0	1.2
7	1.1	3.9	4	0	3.8	1.5
8	1.5	3.8	0	3.1	4	1.7
9	1.5	4	3.6	2.8	0	1.1
10	1.3	3.2	3.5	0	3.6	1.2

The personal preferences of the residents are summarized in Table 4.2, where, the lower bound of each resident is the sum of the power rating of the critical load and the highest priority loads of the residents.

The priority list of the appliances for each house is presented in Table 4.3.

For the experiment, the time duration of each DRR is set to five minutes. The advantage of using this time interval is to prevent the discomfort caused by performing a single DRR with a long time period. At the beginning of each short DRR, the sensor of each house sends the feedbacks to the CEMS which information help the CEMS to optimize the system based on the resident's preferences.

Table 4.2. Personal Preferences of the Ten Residents.

House No.	Highest Priority with AC & EWH	Total Power Rating (kW)	Lower Bound (kW)	Com
1	CD	17.3	10.4	0
2	0	13.3	6.90	1
3	DW	17.4	9.80	0
4	0	9.30	6.70	0
5	0	12.80	6.10	1
6	CD	12.60	9.80	1
7	EV	14.30	10.60	0
8	0	14.10	7.20	1
9	DW	13	9.70	0
10	0	12.80	6.00	1

Table 4.3. The Priority of the Appliances for Ten Residents.

House No.	AC	EWH	CD	DW	EV	CLs
1	2	3	4	6	5	1
2	2	3	5	4	6	1
3	2	3	5	4	6	1
4	2	3	6	4	5	1
5	2	3	4	6	5	1
6	2	3	4	5	6	1
7	2	3	5	6	4	1
8	2	3	6	4	5	1
9	2	3	5	4	6	1
10	2	3	4	6	5	1

For the proposed approach, the reward rates R_1, R_2 and R_3 are set to 20, 40, and 60 cents/ (kW.5min), respectively. For the traditional approach, a reward of 40 cents/ (kW.5min) is used which is the median value of the proposed reward rates. Simulation results are presented in the rest of this section.

4.6.1 DRR1: Approximately 40% demand reduction

In this experiment, the utility sent 55 kW DRR to the CEMS for 20 minutes which is approximately 40% of the total power demand of the community. The results of the

residents' comfort level and the reward distributions are shown in Table 4.4 where the comfort percentage (%) is representing the percentage of time when the power consumption was within the residents' comfortable ranges.

Table 4.4. DRR1 Results for Ten Residents.

House No.	Average Power Consumption (kW)	Comfort Percentage (%)	Rate	Rewards ($)
1	11.525	100	R_1	4.62
2	7.875	100	R_1	4.82
4	3.90	100	R_1	4.32
5	7.50	100	R_1	4.24
6	8.85	100	R_1	3.00
7	9.35	100	R_1	3.96
8	5.30	100	R_1	7.04
9	7.675	100	R_1	4.26
10	6.825	100	R_1	4.78

The results shows that all the residents' were within their comfortable power consumption ranges. Since, the comfort percentage is found 100% for all houses, all houses are rewarded at R_1 rate. House 8 received the most financial rewards, due to the resident's broad comfortable power range means the difference between the total power rating (kW) and the lower bound (kW) is higher than others.

The results are compared with the existing framework in terms of number of active appliances. The results are illustrated in Figure 4.4. In each time step, the proposed approach outperformed the existing framework. For example, at time step 5 minutes, the number of active appliances for the proposed approach is found as 49 where the number of active appliances for the existing framework is found as 41. The results show that the proposed approach is distributed the available energy to the residential appliances more efficiently than the existing framework.

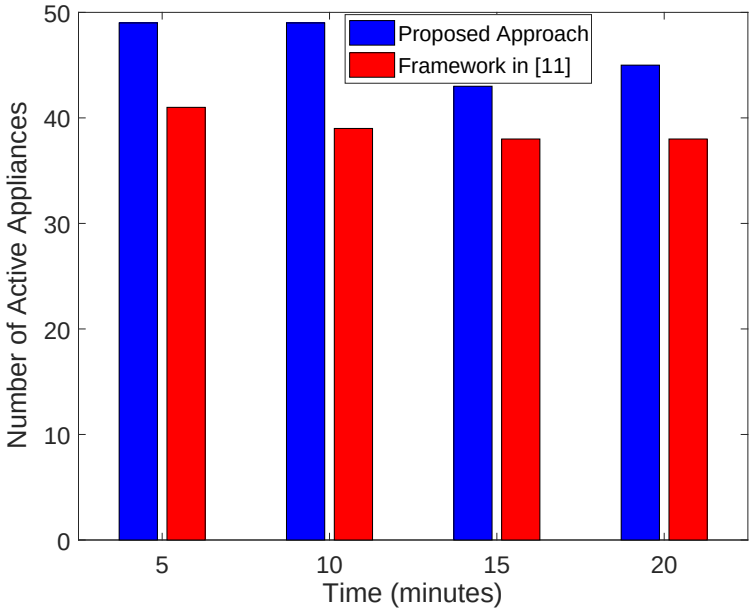

Figure 4.4. Number of active appliances for 40% load curtailment (55 kW).

4.6.2 DRR2: Approximately 55% demand reduction

In this case, the utility sent 75.30 kW DRR to the CEMS for 20 minutes which is approximately 55% of the total power demand of the community. The results of the residents' comfort level and the reward distributions are shown in Table 4.5.

Table 4.5. DRR2 Results for Ten Residents.

House No.	Average Power Consumption (kW)	Comfort Percentage (%)	Rate	Rewards ($)
1	9.35	100	R_1	6.36
2	5.35	100	R_1	6.36
3	8.525	100	R_1	7.10
4	3.90	100	R_1	4.32
5	3.25	75	R_1, R_2	9.86
6	6.825	75	R_1, R_2	6.80
7	9.35	100	R_1	3.96
8	2.85	100	R_1	9.00
9	7.675	100	R_1	4.26
10	3.425	100	R_1	7.50

According to the results, during the 20 minutes of the time period, the comfort indicator values for houses 5 and 6 were higher than 1 in two different five minutes of time interval, respectively. The CEMS allocated higher incentives at R_2 rate to them at that time step, since, both of them are agreed to compromise. The result comparison in terms of number of active appliances are presented in Figure 4.5. Like DRR1, the number of active appliances using the proposed approach is found higher than the existing framework in every time steps. According to the results, it can be concluded that the proposed approach is allocated residential energy to the appliances more efficiently than the existing approach. Further result comparisons are presented next sub-section.

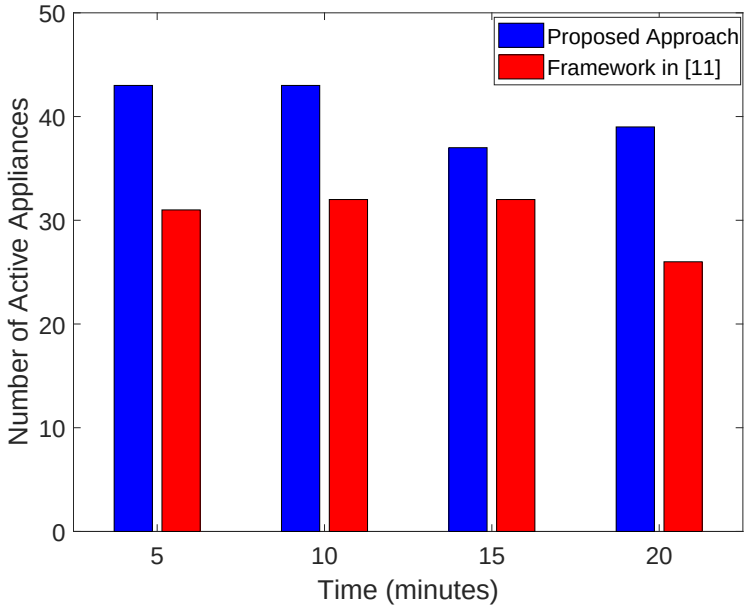

Figure 4.5. Number of active appliances for 55% load curtailment (75.30 kW).

4.6.3 Results Comparison

The results obtained from the proposed approach are compared with the existing framework and the conventional IBDR program techniques in terms of the total financial

rewards in dollars and the average comfortableness in percentages. According to the results, the proposed approach has the following advantages: 1) It significantly increases the average comfort levels during DR events; 2) for both cases, it significantly reduces the reward cost of the utility; 3) it rewarded the residents according to their actual contributions in the DR events. The result comparisons in terms of average comfortableness are shown in Figure 4.6. For both cases, the proposed approach outperformed the existing approaches. The result comparisons in terms of total financial rewards are presented in Figure 4.7. According to the figure, the increase in DRR may lead to a dramatic rise in terms of reward costs. Because, for a large amount of load curtailment, the CEMS has no way without violating some residents' comfort levels to reduce enough demand. The affected residents will be rewarded at R_2 or R_3 rate which increases the total reward cost. For 40% of load curtailment, the existing framework showed competitive performance with the proposed approach, however, the proposed approach showed better performance than the existing approaches. The proposed approach also showed better performance in terms of total financial rewards for 55% of load curtailment.

The proposed approach is also tested for different DRRs with different time lengths using the ten residents system and compared with the existing framework. The three dimensional results for the existing framework and the proposed approach are illustrated in terms of total financial reward and the average comfortableness in Figure 4.8 and 4.9.

The results show that, for both approaches, with the increase of time lengths and the amount of the DRR, the resident comfort levels dramatically fall while the total reward costs rise sharply. According to the results, upto 20% of demand reduction rate, both

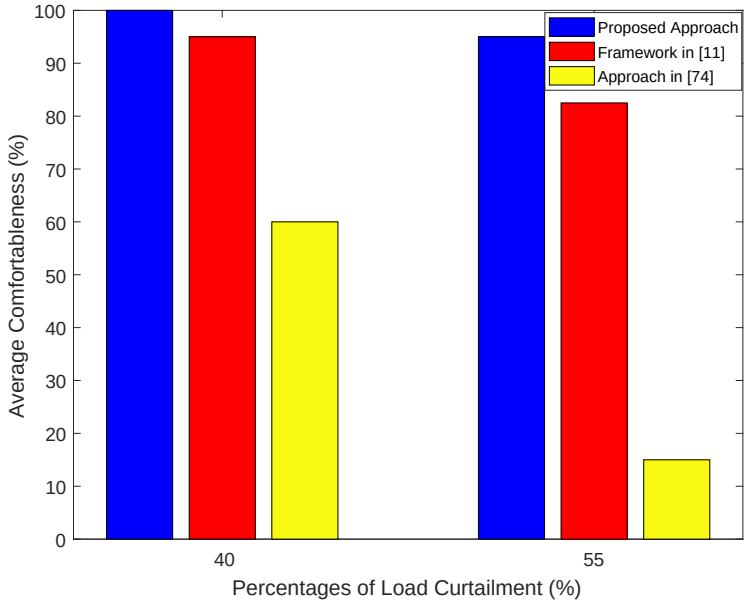

Figure 4.6. Result comparison in terms of average comfortableness.

approaches performed same. However, with the increment of load curtailments and time lengths, the difference between the approaches are observed. For example, for the proposed approach, the maximum financial reward and the minimum average comfortableness for the 60% of load curtailment are observed as $246.16 and 86.67%, respectively, where, for the existing framework, the maximum financial reward and the minimum average comfortableness are experienced as $346.44 and 55%, respectively. According to the results, for all other cases, the proposed approach outperformed the existing framework.

4.6.4 The Performance of a 100-Residents System

The proposed approach is also tested for large resident system where 100 residents are taken into consideration. The power rating ranges for each appliances are summarized in Table 4.6 [11], [33], [52], [75], [79].

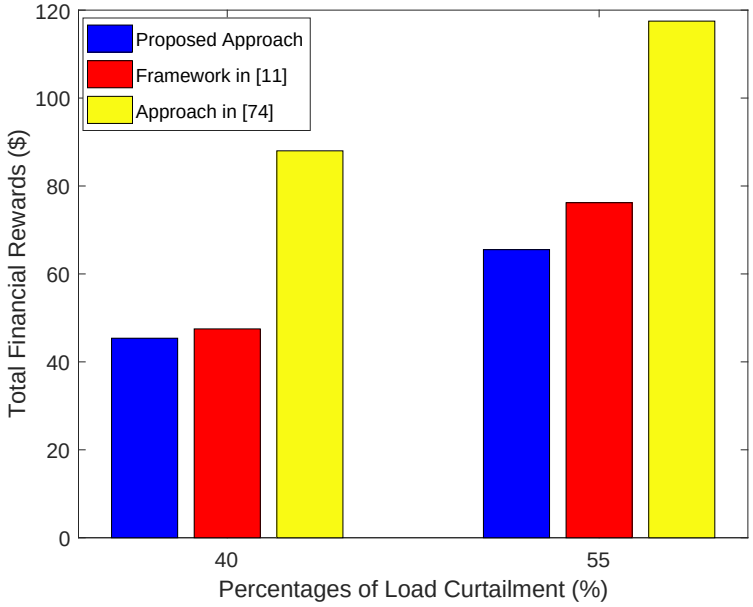

Figure 4.7. Result comparison in terms of total financial rewards.

Table 4.6. Power Rating Ranges of Each Appliance.

Appliances	Power Rating (kW)
Air conditioner	1.1-1.6
Water heater	3.2-4.5
Dish washer	1.8-3.1
Cloth dryer	3.4-4.1
Electric vehicle	3.6-4
Critical loads	1-2

In this experiment, the simulation is conducted for two hundred iterations. For each iteration, the power rating of the appliances are generated randomly within the defined ranges for 100 houses and the total financial rewards as well as the average comfortableness are calculated. After two hundred iterations, the statistical estimated value of the total financial rewards and average comfortableness are obtained as Monte Carlo simulation technique in [80]. The results in terms of both average comfortableness and total financial rewards for proposed approach are presented in Figure 4.10 where different demand reduction rates with different time lengths are taken into consideration.

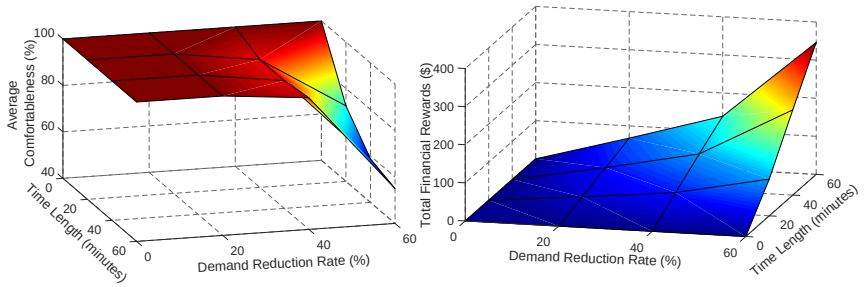

Figure 4.8. Average comfortableness and total financial rewards for different DRR with different time length using the existing framework [11].

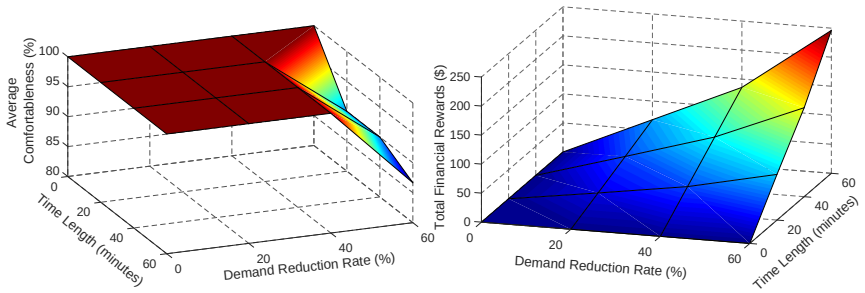

Figure 4.9. Average comfortableness and total financial rewards for different DRR with different time length using the proposed approach.

According to Figure 4.10, for average comfortableness, no effect is observed upto 40% of load curtailment with different time lengths. However, the resident comfort levels dramatically fall for 60% of load curtailment and the level of the resident comfort decreases with the increment of the time length. Again, the total financial rewards of the system increases sharply as the time length and the demand reduction rate increases. For comparison, the results of the existing framework are illustrated in Figure 4.11. According to the results, the proposed approach outperformed the existing framework in terms of both average comfortableness and total financial rewards of the system.

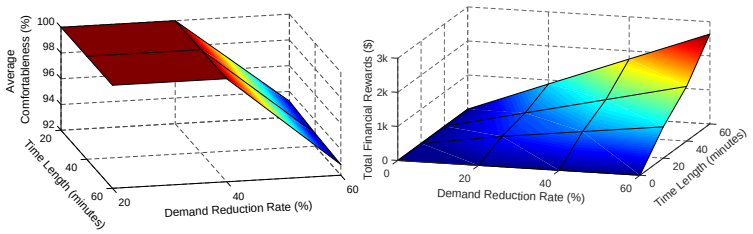

Figure 4.10. Average comfortableness and total financial rewards for different DRR with different time length using the proposed approach for 100-residents system.

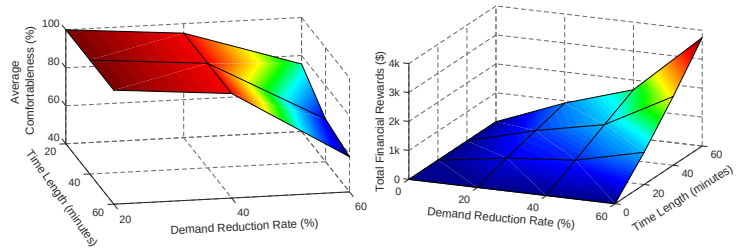

Figure 4.11. Average comfortableness and total financial rewards for different DRR with different time length using the existing framework [11] for 100-residents system.

4.7 Summary

In this section, a residential community energy management system is proposed to manage demand reduction requests efficiently without affecting consumers' comfort levels, and meanwhile reward consumers with financial incentives. A multilevel reward system was developed to satisfy the needs for various types of consumers. The concept of comfort indicator was proposed to measure the comfort level of the residents where both thermal and other electric appliances are taken under consideration. The performance of

the proposed optimization scheme was validated using different demand reduction requests with different time length for both 10-houses and 100-houses simulation studies. The results were compared with the conventional techniques and the proposed approach outperformed the conventional techniques in terms of both total reward cost of the utility and average comfortableness of the residents in the community.

CHAPTER 5 CONCLUSIONS AND FUTURE WORK

5.1 Conclusions and Discussions

Due to environmental concerns and energy crisis, distributed energy sources are accepted as an environmentally and economically beneficial solution for the future. However, increasing penetration of intermittent and variable renewable energy sources has significantly complicated power grid operations. The uncertain nature of renewable energy sources may cause increased operating costs for committing costly reserve units or penalty costs for curtailing load demands. This thesis has focused on the power system optimization of the power grid from three different perspectives.

First, as a viable solution, integration of battery energy storage system has studied. near optimal operation of battery energy storage system has discussed with the presence of wind energy, load demand and power grid by considering lifetime characteristics. The problem has formulated as a Markov decision process, and the near optimal policy has simulated by proposed approximate dynamic programming. To verify the performance of the proposed algorithm, dynamic programming has used to statistically estimate the optimal value of the total system revenue and compared with the proposed approximate dynamic programming approach. The proposed approximate dynamic programming approach successfully approximated the solution that was very close to the optimal solution of dynamic programming. Simulation studies have been carried out for three cases: ten different stochastic test problems were investigated and validated with dynamic programming, one stochastic test problem is used by varying battery SOC_{stp} to see the effect of battery *SOC* on the total system revenue and for further analysis real-time pricing

was also used. The simulation results have shown that approximate dynamic programming is a powerful tool for the power system optimization problem that can provide sequential optimal decision and control to address optimal operation of BESS.

Second, the optimal operation of energy systems in an islanded microgrid has investigated considering battery lifetime characteristics. Extensive simulations were conducted to validate the effectiveness of the proposed approximate dynamic programming approach. The traditional linear programming and dynamic programming were used for the deterministic and stochastic case study, respectively. Simulation results showed that the ADP can achieve 100% for deterministic case study and at least 98% of optimality for stochastic case study with lower computational time, respectively. Yearly simulation results were presented to estimate the net savings of the system for different SOC setups in the control strategy. Moreover, the proposed approximate dynamic programming approach was validated for different data samples. The results showed that the proposed approximate dynamic programming approach outperformed the traditional dynamic programming approach with the increasing number of data samples. According to the results, the proposed approximate dynamic programming approach is a computationally efficient tool for the power system optimization problems.

Third, another widely used power system optimization technique named demand side management has studied. A residential energy management system has proposed for aggregating residential demands. In the proposed strategy, the residential energy management system serves as an agent of the utility. The role of the proposed optimization scheme is not only to distribute demand reduction request by the utility among residential appliances quickly and efficiently without affecting residents' comfort

levels but also to strategically reward the residents for their participation. A multilevel reward system was developed to satisfy the needs for various types of consumers. The concept of comfort indicator was proposed to measure the comfort level of the residents. The performance of the proposed optimization scheme was validated using different demand reduction requests with different time length for both 10-houses and 100-houses simulation studies. The results were compared with two existing techniques and the proposed approach outperformed those techniques in terms of both total reward cost of the utility and average comfortableness of the residents in the community.

5.2 Future Work

The future work along this direction includes the following major tasks:

1. For the proposed approximate dynamic programming approach, harmonic step size is used to smooth the value function approximation. In existing literature, different stochastic filters are reported for the design of the step size. The potential barrier of using the harmonic step size filter is the tuning parameter, which needs to be adjusted based on the specific problem. This issue can possibly be addressed by using the bias-adjusted Kalman filter, which adjusts itself to the actual behavior of the algorithm. In the future, the bias-adjusted Kalman filter can be investigated as well as other stochastic filters to find the improvement of the proposed ADP approach.

2. Analyze the effect of integration of multiple distributed energy resources like solar, wind, hydro, etc. for investigating the stochastic effect on the optimization and evaluate the performance of the proposed approximate dynamic programming

approach to solve this problem.

3. The proposed ADP can be compared with the other existing approaches to investigate the performance of the algorithm for power system optimization problems. Another interesting direction is to investigate the proposed ADP approach for different real-time BESSs for the comparative study.

4. Test the proposed residential energy management system for large resident system and evaluate the performance of the proposed strategy in terms of total reward cost and the average comfortableness of the community.

In general, all these works are expected to enhance the power system quality, stability and reliability.

LITERATURE CITED

[1] P. Li, D. Xu, Z. Zhou, W.-J. Lee, and B. Zhao, "Stochastic optimal operation of microgrid based on chaotic binary particle swarm optimization," *IEEE Transactions on Smart Grid*, vol. 7, no. 1, pp. 66–73, 2016.

[2] F. Katiraei and M. R. Iravani, "Power management strategies for a microgrid with multiple distributed generation units," *IEEE transactions on power systems*, vol. 21, no. 4, pp. 1821–1831, 2006.

[3] T. A. Nguyen and M. Crow, "Stochastic optimization of renewable-based microgrid operation incorporating battery operating cost," *IEEE Transactions on Power Systems*, vol. 31, no. 3, pp. 2289–2296, 2016.

[4] W. Su, J. Wang, and J. Roh, "Stochastic energy scheduling in microgrids with intermittent renewable energy resources," *IEEE Transactions on Smart Grid*, vol. 5, no. 4, pp. 1876–1883, 2014.

[5] L. I. Minchala-Avila, L. Garza-Castañón, Y. Zhang, and H. J. A. Ferrer, "Optimal energy management for stable operation of an islanded microgrid," *IEEE Transactions on Industrial Informatics*, vol. 12, no. 4, pp. 1361–1370, 2016.

[6] X. Luo, J. Wang, M. Dooner, and J. Clarke, "Overview of current development in electrical energy storage technologies and the application potential in power system operation," *Applied Energy*, vol. 137, pp. 511–536, 2015.

[7] H. Chen, T. N. Cong, W. Yang, C. Tan, Y. Li, and Y. Ding, "Progress in electrical energy storage system: A critical review," *Progress in Natural Science*, vol. 19, no. 3, pp. 291–312, 2009.

[8] S. Chalise, J. Sternhagen, T. M. Hansen, and R. Tonkoski, "Energy management of remote microgrids considering battery lifetime," *The Electricity Journal*, vol. 29, no. 6, pp. 1–10, 2016.

[9] L. Gelazanskas and K. A. Gamage, "Demand side management in smart grid: A review and proposals for future direction," *Sustainable Cities and Society*, vol. 11, pp. 22–30, 2014.

[10] U. E. I. Administration, "Monthly energy review," p. 109, Apr. 2014.

[11] Q. Hu, F. Li, X. Fang, and L. Bai, "A framework of residential demand aggregation with financial incentives," *IEEE Transactions on Smart Grid*, 2016.

[12] Q Qdr, "Benefits of demand response in electricity markets and recommendations for achieving them," *US department of energy*, 2006.

[13] A. Chaouachi, R. M. Kamel, R. Andoulsi, and K. Nagasaka, "Multiobjective intelligent energy management for a microgrid," *IEEE Transactions on Industrial Electronics*, vol. 60, no. 4, pp. 1688–1699, 2013.

[14] C. Chen, S. Duan, T. Cai, B. Liu, and G. Hu, "Smart energy management system for optimal microgrid economic operation," *IET renewable power generation*, vol. 5, no. 3, pp. 258–267, 2011.

[15] S. Chen and H. B. Gooi, "Jump and shift method for multi-objective optimization," *IEEE Transactions on Industrial Electronics*, vol. 58, no. 10, pp. 4538–4548, 2011.

[16] W. Su, Z. Yuan, and M.-Y. Chow, "Microgrid planning and operation: Solar energy and wind energy," in *Power and Energy Society General Meeting, 2010 IEEE*, IEEE, 2010, pp. 1–7.

[17] J. Wang, C. Liu, D. Ton, Y. Zhou, J. Kim, and A. Vyas, "Impact of plug-in hybrid electric vehicles on power systems with demand response and wind power," *Energy Policy*, vol. 39, no. 7, pp. 4016–4021, 2011.

[18] B. Zhao, X. Zhang, J. Chen, C. Wang, and L. Guo, "Operation optimization of standalone microgrids considering lifetime characteristics of battery energy storage system," *IEEE Transactions on Sustainable Energy*, vol. 4, no. 4, pp. 934–943, 2013.

[19] S. Chakraborty, M. D. Weiss, and M. G. Simoes, "Distributed intelligent energy management system for a single-phase high-frequency ac microgrid," *IEEE Transactions on Industrial electronics*, vol. 54, no. 1, pp. 97–109, 2007.

[20] R. Palma-Behnke, C. Benavides, F. Lanas, B. Severino, L. Reyes, J. Llanos, and D. Sáez, "A microgrid energy management system based on the rolling horizon strategy," *IEEE Transactions on Smart Grid*, vol. 4, no. 2, pp. 996–1006, 2013.

[21] S. Moazeni, W. B. Powell, and A. H. Hajimiragha, "Mean-conditional value-at-risk optimal energy storage operation in the presence of transaction costs," *IEEE Transactions on Power Systems*, vol. 30, no. 3, pp. 1222–1232, 2015.

[22] M. L. Di Silvestre, G. Graditi, and E. R. Sanseverino, "A generalized framework for optimal sizing of distributed energy resources in micro-grids using an indicator-based swarm approach," *IEEE Transactions on Industrial Informatics*, vol. 10, no. 1, pp. 152–162, 2014.

[23] C. Chen, S. Duan, T. Cai, B. Liu, and G. Hu, "Optimal allocation and economic analysis of energy storage system in microgrids," *IEEE Transactions on Power Electronics*, vol. 26, no. 10, pp. 2762–2773, 2011.

[24] C. Liu, J. Wang, A. Botterud, Y. Zhou, and A. Vyas, "Assessment of impacts of phev charging patterns on wind-thermal scheduling by stochastic unit commitment," *IEEE Transactions on Smart Grid*, vol. 3, no. 2, pp. 675–683, 2012.

[25] J Wang, A Botterud, R Bessa, H Keko, L Carvalho, D Issicaba, J Sumaili, and V Miranda, "Wind power forecasting uncertainty and unit commitment," *Applied Energy*, vol. 88, no. 11, pp. 4014–4023, 2011.

[26] R. Jiang, J. Wang, and Y. Guan, "Robust unit commitment with wind power and pumped storage hydro," *IEEE Transactions on Power Systems*, vol. 27, no. 2, pp. 800–810, 2012.

[27] Q. Wang, Y. Guan, and J. Wang, "A chance-constrained two-stage stochastic program for unit commitment with uncertain wind power output," *IEEE Transactions on Power Systems*, vol. 27, no. 1, pp. 206–215, 2012.

[28] A. A. ElDesouky, "Security and stochastic economic dispatch of power system including wind and solar resources with environmental consideration," *International Journal of Renewable Energy Research (IJRER)*, vol. 3, no. 4, pp. 951–958, 2013.

[29] T. A. Nguyen, X. Qiu, J. D. Guggenberger II, M. L. Crow, and A. C. Elmore, "Performance characterization for photovoltaic-vanadium redox battery microgrid systems," *IEEE Transactions on Sustainable Energy*, vol. 5, no. 4, pp. 1379–1388, 2014.

[30] Y. Tan, Y. Cao, C. Li, Y. Li, L. Yu, Z. Zhang, and S. Tang, "Microgrid stochastic economic load dispatch based on two-point estimate method and improved particle swarm optimization," *International Transactions on Electrical Energy Systems*, vol. 25, no. 10, pp. 2144–2164, 2015.

[31] S. Mohammadi, S. Soleymani, and B. Mozafari, "Scenario-based stochastic operation management of microgrid including wind, photovoltaic, micro-turbine, fuel cell and energy storage devices," *International Journal of Electrical Power & Energy Systems*, vol. 54, pp. 525–535, 2014.

[32] T. Niknam, R. Azizipanah-Abarghooee, and M. R. Narimani, "An efficient scenario-based stochastic programming framework for multi-objective optimal micro-grid operation," *Applied Energy*, vol. 99, pp. 455–470, 2012.

[33] Z. Chen, L. Wu, and Y. Fu, "Real-time price-based demand response management for residential appliances via stochastic optimization and robust optimization," *IEEE Transactions on Smart Grid*, vol. 3, no. 4, pp. 1822–1831, 2012.

[34] N. Growe-Kuska, H. Heitsch, and W. Romisch, "Scenario reduction and scenario tree construction for power management problems," in *Power tech conference proceedings, 2003 IEEE Bologna*, IEEE, vol. 3, 2003, 7–pp.

[35] L. Wu, M. Shahidehpour, and T. Li, "Cost of reliability analysis based on stochastic unit commitment," *IEEE Transactions on Power Systems*, vol. 23, no. 3, pp. 1364–1374, 2008.

[36] A. Papavasiliou, S. S. Oren, and R. P. O'Neill, "Reserve requirements for wind power integration: A scenario-based stochastic programming framework," *IEEE Transactions on Power Systems*, vol. 26, no. 4, pp. 2197–2206, 2011.

[37] M. Hassan and M. Abido, "Optimal design of microgrids in autonomous and grid-connected modes using particle swarm optimization," *IEEE Transactions on power electronics*, vol. 26, no. 3, pp. 755–769, 2011.

[38] S. A. Pourmousavi, M. H. Nehrir, C. M. Colson, and C. Wang, "Real-time energy management of a stand-alone hybrid wind-microturbine energy system using particle swarm optimization," *IEEE Transactions on Sustainable Energy*, vol. 1, no. 3, pp. 193–201, 2010.

[39] A. Litchy and M. Nehrir, "Real-time energy management of an islanded microgrid using multi-objective particle swarm optimization," in *2014 IEEE PES General Meeting— Conference & Exposition*, IEEE, 2014, pp. 1–5.

[40] M. A. A. Pedrasa, T. D. Spooner, and I. F. MacGill, "Scheduling of demand side resources using binary particle swarm optimization," *IEEE Transactions on Power Systems*, vol. 24, no. 3, pp. 1173–1181, 2009.

[41] D. R. Jiang, T. V. Pham, W. B. Powell, D. F. Salas, and W. R. Scott, "A comparison of approximate dynamic programming techniques on benchmark energy storage problems: Does anything work?" In *Adaptive Dynamic Programming and Reinforcement Learning (ADPRL), 2014 IEEE Symposium on*, IEEE, 2014, pp. 1–8.

[42] W. B. Powell, *Approximate Dynamic Programming: Solving the Curses of Dimensionality*. 2011.

[43] J. Si, A. Barto, W. Powell, and D. Wunsch, Eds., *Handbook of learning and approximate dynamic programming*. John Wiley & Sons, 2004.

[44] L. Hannah and D. B. Dunson, "Approximate dynamic programming for storage problems," in *Proceedings of the 28th International Conference on Machine Learning (ICML-11)*, 2011, pp. 337–344.

[45] D. F. Salas and W. B. Powell, "Benchmarking a scalable approximate dynamic programming algorithm for stochastic control of multidimensional energy storage problems," *Dept. Oper. Res. Financial Eng., Princeton Univ., Princeton, NJ, USA*, 2013.

[46] Z. Ni, Y. Tang, X. Sui, H. He, and J. Wen, "An adaptive neuro-control approach for multi-machine power systems," *International Journal of Electrical Power & Energy Systems*, vol. 75, pp. 108–116, 2016.

[47] Y. Tang, H. He, Z. Ni, J. Wen, and T. Huang, "Adaptive Modulation for DFIG and STATCOM With High-Voltage Direct Current Transmission," *IEEE Transactions on Neural Networks and Learning Systems*, vol. 27, pp. 1762–1772, 8 Aug. 2016.

[48] C. Vivekananthan, Y. Mishra, G. Ledwich, and F. Li, "Demand response for residential appliances via customer reward scheme," *IEEE transactions on smart grid*, vol. 5, no. 2, pp. 809–820, 2014.

[49] K. M. Tsui and S.-C. Chan, "Demand response optimization for smart home scheduling under real-time pricing," *IEEE Transactions on Smart Grid*, vol. 3, no. 4, pp. 1812–1821, 2012.

[50] A.-H. Mohsenian-Rad and A. Leon-Garcia, "Optimal residential load control with price prediction in real-time electricity pricing environments," *IEEE transactions on Smart Grid*, vol. 1, no. 2, pp. 120–133, 2010.

[51] N. Li, L. Chen, and S. H. Low, "Optimal demand response based on utility maximization in power networks," in *Power and Energy Society General Meeting, 2011 IEEE*, IEEE, 2011, pp. 1–8.

[52] M. Pipattanasomporn, M. Kuzlu, and S. Rahman, "An algorithm for intelligent home energy management and demand response analysis," *IEEE Transactions on Smart Grid*, vol. 3, no. 4, pp. 2166–2173, 2012.

[53] J. M. Lujano-Rojas, C. Monteiro, R. Dufo-Lopez, and J. L. Bernal-Agustín, "Optimum residential load management strategy for real time pricing (rtp) demand response programs," *Energy Policy*, vol. 45, pp. 671–679, 2012.

[54] Z. Zhao, W. C. Lee, Y. Shin, and K.-B. Song, "An optimal power scheduling method for demand response in home energy management system," *IEEE Transactions on Smart Grid*, vol. 4, no. 3, pp. 1391–1400, 2013.

[55] F. E. R. Commission *et al.*, *Federal energy regulatory commission assessment of demand response & advanced metering, staff report and excel data, december 29. 2008*, 2008.

[56] C. Kang and W. Jia, "Transition of tariff structure and distribution pricing in china," in *Power and Energy Society General Meeting, 2011 IEEE*, IEEE, 2011, pp. 1–5.

[57] H. Zhong, L. Xie, and Q. Xia, "Coupon incentive-based demand response: Theory and case study," *IEEE Transactions on Power Systems*, vol. 28, no. 2, pp. 1266–1276, 2013.

[58] P. Cappers, C. Goldman, and D. Kathan, "Demand response in us electricity markets: Empirical evidence," *Energy*, vol. 35, no. 4, pp. 1526–1535, 2010.

[59] X. Fang, Q. Hu, F. Li, B. Wang, and Y. Li, "Coupon-based demand response considering wind power uncertainty: A strategic bidding model for load serving entities," *IEEE Transactions on Power Systems*, vol. 31, no. 2, pp. 1025–1037, 2016.

[60] X. Fang, F. Li, Q. Hu, and Y. Wei, "Strategic cbdr bidding considering ftr and wind power," *IET Generation, Transmission & Distribution*, vol. 10, no. 10, pp. 2464–2474, 2016.

[61] D. S. Callaway, "Tapping the energy storage potential in electric loads to deliver load following and regulation, with application to wind energy," *Energy Conversion and Management*, vol. 50, no. 5, pp. 1389–1400, 2009.

[62] C. Perfumo, E. Kofman, J. H. Braslavsky, and J. K. Ward, "Load management: Model-based control of aggregate power for populations of thermostatically controlled loads," *Energy Conversion and Management*, vol. 55, pp. 36–48, 2012.

[63] M. A. F. Ghazvini, P. Faria, S. Ramos, H. Morais, and Z. Vale, "Incentive-based demand response programs designed by asset-light retail electricity providers for the day-ahead market," *Energy*, vol. 82, pp. 786–799, 2015.

[64] M. A. F. Ghazvini, J. Soares, N. Horta, R. Neves, R. Castro, and Z. Vale, "A multi-objective model for scheduling of short-term incentive-based demand response programs offered by electricity retailers," *Applied Energy*, vol. 151, pp. 102–118, 2015.

[65] P. Siano, "Demand response and smart grids—a survey," *Renewable and Sustainable Energy Reviews*, vol. 30, pp. 461–478, 2014.

[66] D. Jenkins, J Fletcher, and D. Kane, "Lifetime prediction and sizing of lead-acid batteries for microgeneration storage applications," *IET Renewable Power Generation*, vol. 2, no. 3, pp. 191–200, 2008.

[67] D. R. Jiang and W. B. Powell, "An approximate dynamic programming algorithm for monotone value functions," *Operations Research*, vol. 63, no. 6, pp. 1489–1511, 2015.

[68] A. Das, Z. Ni, M. T. Hansen, and X. Zhong, "Energy storage system operation: Case studies in deterministic and stochastic environments," in *2016 IEEE PES Innovative Smart Grid Technologies*, IEEE, 2016, pp. 1–5.

[69] (2016). Live Prices https://hourlypricing.comed.com/live-prices/, [Online]. Available: https://hourlypricing.comed.com/live-prices/ (visited on 04/01/2016).

[70] Y. Tang, H. He, Z. Ni, and J. Wen, "Optimal operation for energy storage with wind power generation using adaptive dynamic programming," in *2015 IEEE Power & Energy Society General Meeting*, IEEE, 2015, pp. 1–6.

[71] A. Das, Z. Ni, and X. Zhong, "Near optimal control for microgrid energy systems considering battery lifetime characteristics," in *2016 IEEE Symposium Series on Computational Intelligence (IEEE SSCI 2016)*, IEEE, 2016, pp. 1–7.

[72] R. J. Vanderbei, *Linear Programming: Foundations and Extensions (Second Edition)*. Springer, 2015.

[73] R. Dufo-López and J. L. Bernal-Agustín, "Multi-objective design of pv-wind-diesel-hydrogen-battery systems," *Renewable energy*, vol. 33, no. 12, pp. 2559–2572, 2008.

[74] T. Anandalaskhmi, S. Sathiakumar, and N. Parameswaran, "Peak reduction algorithms for a smart community," in *International Conference on Energy Efficient Technologies for Sustainability (ICEETS)*, IEEE, 2013, pp. 1113–1119.

[75] S. T. I. Muhandiram Arachchige, "Home energy management system: A home energy management system under different electricity pricing mechanisms," Master's thesis, Universitetet i Agder; University of Agder, 2014.

[76] S. Shao, M. Pipattanasomporn, and S. Rahman, "Development of physical-based demand response-enabled residential load models," *IEEE Transactions on power systems*, vol. 28, no. 2, pp. 607–614, 2013.

[77] T. Roy, A. Das, and Z. Ni, "Optimization in load scheduling of a residential community using dynamic pricing," in *2016 IEEE PES Innovative Smart Grid Technologies (ISGT)*, IEEE, 2016, pp. 1–5.

[78] J. Fortuny-Amat and B. McCarl, "A representation and economic interpretation of a two-level programming problem," *Journal of the operational Research Society*, pp. 783–792, 1981.

[79] J. Kondoh, N. Lu, and D. J. Hammerstrom, "An evaluation of the water heater load potential for providing regulation service," in *Power and Energy Society General Meeting, 2011 IEEE*, IEEE, 2011, pp. 1–8.

[80] A. Shapiro and A. Philpott, "A tutorial on stochastic programming," *Manuscript. Available at www2. isye. gatech. edu/ashapiro/publications. html*, vol. 17, 2007.